UNCLASSIFIED
UNLIMITED

National Research Council Canada
Conseil national de recherches Canada

NATIONAL AERONAUTICAL ESTABLISHMENT

LABORATORY TECHNICAL REPORT

LTR - ST - 1651

THE RELIABILTY AND SENSITIVITY OF NDI TECHNIQUES IN DETECTING LCF CRACKS IN FASTENER BOLT HOLES OF COMPRESSOR DISCS

N.C. BELLINGER, A. FAHR, A.K. KOUL, G. GOULD AND P. STOUTE

RAPPORT TECHNIQUE DE LABORATOIRE

ÉTABLISSEMENT AÉRONAUTIQUE NATIONAL

25 FEBRUARY 1988

OTTAWA, CANADA

National Research Council Canada
Conseil national de recherches Canada

National Aeronautical Establishment
Établissement aéronautique national

Laboratory Report

Rapport Laboratoire

REPORT / RAPPORT: LTR-ST-1651

DATE: 25 February 1988

LAB. ORDER / COMM. LAB.:

CLASSIFICATION: Unclassified

DISTRIBUTION: Unlimited

FOR / POUR: Research carried out under Structures and Materials Laboratory Project 07317: Aerospace Metallic Materials, and supported by the Chief, Research and Development, National Defence under

REFERENCE / REFERENCE: Financial Agreement 2207325F084: Development of Gas Turbine Engine Structures and Materials Technology Base.

LTR-ST-1651

THE RELIABILITY AND SENSITIVITY OF NDI TECHNIQUES IN DETECTING LCF CRACKS IN FASTENER BOLT HOLES OF COMPRESSOR DISCS

SUBMITTED BY / PRESENTÉ PAR: W. Wallace
LABORATORY HEAD / CHEF DE LABORATOIRE

APPROVED / APPROUVÉ: G.F. Marsters
DIRECTOR / DIRECTEUR

AUTHOR / AUTEUR: N.C. Bellinger *, A. Fahr, A.K. Koul, G. Gould*, P. Stoute *

*Carleton University, Ottawa

THIS REPORT MAY NOT BE PUBLISHED WHOLLY OR IN PART WITHOUT THE WRITTEN CONSENT OF THE NATIONAL AERONAUTICAL ESTABLISHMENT

CE RAPPORT NE DOIT PAS ÊTRE REPRODUIT NI EN ENTIER NI EN PARTIE SANS UNE AUTORISATION ÉCRITE DE L'ÉTABLISSEMENT AÉRONAUTIQUE NATIONAL

Structures and Materials Laboratory
Laboratoire des structures et des matériaux

CONTENTS

		Page
	ABSTRACT	
1.0	INTRODUCTION	1
2.0	STATISTICAL ANALYSIS OF THE NDI DATA	2
	2.1 Probability of Detection Curves	3
3.0	EXPERIMENTAL MATERIALS AND METHODS	5
	3.1 J85-CAN40 Compressor Discs	5
	3.2 Nondestructive Inspection Techniques	5
	3.2.1 Liquid Penetrant Inspection (LPI)	6
	3.2.2 Eddy Current Inspection (ECI)	7
	3.2.3 Real Time Microfocus X-Radiography	7
	3.2.4 Ultrasonic Leaky Waves Using a C-scan System	8
	3.3 Destructive Crack Verification Procedures	9
4.0	RESULTS	10
	4.1 Histograms	10
	4.2 Probability of Detection Curves and the 90% POD/95% Confidence Lines	10
	4.3 Actual Versus Measured Crack Lengths	11
5.0	DISCUSSION	11
6.0	CONCLUSIONS	13
7.0	ACKNOWLEDGEMENTS	15
8.0	REFERENCES	15
	TABLES	
	FIGURES	
	APPENDIX A	

ABSTRACT

The successful implementation of a damage tolerance based life cycle management methodology is strongly dependent on the sensitivity and reliability of the nondestructive inspection (NDI) technique that is used to inspect the component. A demonstration program has been carried out to characterize the sensitivity and reliability of several NDI techniques in detecting low cycle fatigue (LCF) cracks in the J85-CAN40 fifth stage compressor disc tie bolt holes. The quantitative data on the probability of detection (POD) of LCF cracks were generated for a conventional liquid penetrant inspection (LPI) technique using a range of penetrant soaking times, a manual eddy current inspection technique using two sensitivity levels as well as an ultrasonic leaky wave technique using an automated C-scan system. Different statistical distributions were compared to determine which distribution gives the best 95% lower confidence bound about the mean log-logistic POD line.

The results indicate that amongst the techniques evaluated, the manual eddy current technique is most sensitive in terms of the detection of small cracks whereas the automated ultrasonic leaky wave technique is the most reliable for compressor disc bolt hole cracks.

1.0 INTRODUCTION

It is generally acknowledged that the useful life of aircraft engine components, such as discs and spacers, is not fully utilized through a safe life design approach since only a few (eg. 1 in 1000) components will have developed a crack of detectable size at retirement(1-3). Therefore, alternative design and life cycle management procedures based on damage tolerance concepts are currently being considered for some new and existing engines. In the damage tolerance approach it is assumed that the fracture critical location of a component contains an initial crack of a size that lies just below the detection limit of the nondestructive inspection (NDI) techniques used to inspect the component. It is also assumed that the crack will grow during service in a manner that can be predicted by linear elastic fracture mechanics, or other acceptable methods, until a predetermined crack length limit is reached beyond which the risk of failure due to rapid crack growth becomes excessive(1). This predetermined crack length which is known as the dysfunction limit is usually caclulated using a fracture mechanics analysis and a safety factor and is given by the engine manufacturers. A damage tolerance approach ensures that the initial crack does not grow beyond its dysfunction size by calculating the number of fatigue cycles or hours to dysfunction and imposing inspection intervals shorter than the time interval required for the crack to grow from its initial size to dysfunction.

Irrespective of the damage tolerance approach used to calculate the number of hours (or cycles) to dysfunction, it is quite clear that the predictions will be strongly influenced by the initial and dysfunction crack length values used in the calculations. The dysfunction crack size is analytically determined by using the best estimates of service loads and materials properties using worst case service conditions for a given component. The initial crack length on the other hand, will depend strongly upon the detection and sizing capabilities of nondestructive inspection (NDI) technique used to inspect the components. This dependence requires that NDI techniques be quantified in terms of crack detection capability (sensitivity) and reliability (probability of detection) in order to establish the most suitable NDI technique for use in damage tolerance life predictions. One way of assessing the suitability of a given NDI technique is by using a statistically valid demonstration programme in which flawed and flaw free parts are inspected by NDI procedures that duplicate proposed maintenance inspections. The objective of such a programme would be to establish the sensitivity and reliability of NDI procedures for a given part and flaw size.

As part of the overall NAE research activity in life extension concepts for aircraft

engine discs and spacers, a cooperative project involving NAE, DND and Carleton University was initiated in 1986. The aim of the project was to evaluate the sensitivity and reliability of several NDI techniques in the detection and sizing of low cycle fatigue cracks in the tie bolt holes of J85-CAN40 compressor discs. The NDI techniques were selected from standard military procedures that are presently practiced at the Aircraft Maintenance and Development Unit (AMDU) of the Department of National Defence (DND) for detecting bolt hole cracks as well as newer methods which were available at AMDU and NAE at the time of the investigation. The techniques used included the conventional liquid penetrant inspection (LPI), manual eddy current inspection (ECI), microfocus X-radiography (MXR) and ultrasonic leaky wave (ULW). The ULW inspection was carried out in an automated C-scan system. After inspections, the crack sites were examined by optical as well as scanning electron microscopy.

This report describes the procedures used for the nondestructive and destructive inspections of the compressor discs as well as the statistical analysis used to obtain the probability of detection curves and the 95% lower confidence bounds. The different NDI techniques were compared using a 90% POD/95% confidence limit as well as a 90% POD/mean line limit.

2.0 STATISTICAL ANALYSIS OF THE NDI DATA

There are three categories of experiments which can be used to evaluate the reliability of NDI techniques[4]:

Category 1 - NDI Capability at One Crack Length

This category of experiment can be viewed as a method for demonstrating that an NDI system can detect at least a given percentage of cracks of a specified length with a specified confidence limit. For example, this approach could be used to show that there is 95% confidence that at least 90% of all cracks of length x mm will be found. These experiments have limited use since information is provided only for the crack length inspected.

Category 2 - Estimation of POD with One Observation Per Crack

The majority of experiments fall in this category including this demonstration

programme. Many components covering a range of crack lengths are inspected once and the results are used to estimate the POD as a function of crack length with confidence bounds. Since there are generally not a sufficient number of cracks of the same length, the crack lengths are grouped into intervals of crack length. It is assumed that all cracks within a specified interval have approximately the same POD.

Category 3 - Estimation of the POD with Multiple Observations Per Crack

This category of experiment resulted from a large NDI reliability programme performed by the U.S. Air Force, known as the "Have Cracks Will Travel" programme (Ref. 5), where sections of aircraft airframe were transported to depots and inspected for cracks by personnel using various NDI systems. This method of collecting data provided an estimate of a POD for each individual crack and demonstrated clearly that not all cracks of the same length have the same POD[5].

2.1 Probability of Detection Curves

The binomial distribution has traditionally been used to approximate the probability of detection curves and to specify the confidence bounds for POD values. The POD is defined as the ratio of cracks that will be detected by the NDI technique in question, to the total number of cracks present in the same size range. For both categories 1 and 2, this distribution has been found to fit the observed data better than other curves such as the Chi-square, normal and Poisson distributions[6]. The problem with the binomial distribution is the fact that the confidence bounds are significantly influenced by the method of assigning cracks to an interval and the number of cracks contained in each interval. Also, category 3 type data have demonstrated that cracks of the same length could have different POD values[5] (see Figure 1). Therefore, the binomial distribution is not always suitable for representing the POD values since it assumes that a specific crack length always has the same probability of detection.

Berens and Hovey[4] have examined a number of distributions including Weibull, Probit, log odds-linear scale, and log-logistics in order to determine that which is best for analysis of POD data. By performing an appropriate transformation to the detection probabilities and crack lengths, they carried out a linear regression analysis to determine the consistency of each distribution. Consistency was defined by Berens and Hovey as the

failure to reject the hypothesis at the 0.1 level of significance[4]. It was shown that no other distribution modelled the POD data as consistently as the log-logistic distribution.

The functional form of the log-logistic distribution is as follows[4]:

$$P_i = \frac{\exp(\beta_o + \beta_1 \ln a_i)}{1 + \exp(\beta_o + \beta_1 \ln a_i)} \qquad (1)$$

where P_i = probability of detection

a_i = crack length

β_o = location parameter

β_1 = slope parameter

i = 1 to n, where n = total number of crack size intervals

If the data are of category 3 type, the a_i, P_i data pairs can be input directly into transformations required by the analysis. However, if the data are from category 2, the cracks have to be grouped into intervals of crack length and the proportion of detection assigned to a single crack length representative of the interval. Berens and Hovey have suggested that the middle of each interval would be more representative of the detection probability than the end points.

For linear regression analysis and given n pairs of a_i, P_i data points, the log-logistics transformations can be performed by[4]:

$$y_i = \alpha + \beta x_i$$

where $$y_i = \ln(P_i/(1 - P_i)) \qquad (2)$$

and $$x_i = \ln(a_i) \qquad (3)$$

α and β are respectively the intercept and the slope and are found from linear regression analysis. In those cases for which none or all the cracks are found, values for P_i are defined to be $1/(n + 1)$, or $n/(n + 1)$, respectively.

The log-logistic curve represents the mean POD for a crack length. Standard statistical distributions such as the F-distribution, student t-distribution and normal distribution can then be used to find confidence bounds on the linear regression line based on the log-logistic curve and then transformed back to the POD curve. Figure 2 illustrates a log-logistic curve with a 95% lower confidence bound fitted about it.

3.0 EXPERIMENTAL MATERIALS AND METHODS

3.1 J85-CAN40 Compressor Discs

The J85-CAN40 engine fifth stage compressor disc used in this study is made of AM-355, a precipitation hardened, martensitic stainless steel. Each disc contains forty tie bolt holes which are used to assemble the compressor section. It is already known that low cycle fatigue cracks initiate at these bolt holes and grow radially towards the bore of the disc[7]. Occasionally, however, cracks have been found to grow radially outward. A typical cross section of the fifth stage compressor discs is shown in Figure 3. These discs were chosen for this study because a large number of cracked discs were readily available from the engine overhaul and maintenance contractor (Orenda Division of Hawker-Siddeley Canada). Ten service exposed discs that were likely to contain a maximum number of tie bolt hole cracks were selected for use in the present investigation.

3.2 Nondestructive Inspection Techniques

The discs had been initially inspected under the maintenance contract by Orenda using a liquid penetrant inspection (LPI) technique, and their inspection results were made available to NAE in the form of inspection maps. These discs were then sent to AMDU for nondestructive testing. Two sets of inspections were carried out by AMDU using conventional liquid penetrant methods as well as a manual eddy current technique. Also, microfocus X-radiography was performed on a number of discs at AMDU on a trial basis. Once AMDU inspections were completed, a further inspection was carried out on the discs using the ultrasonic leaky wave method in an automated C-scan system available at NAE. The order in which the different NDI techniques were carried out is shown in the flowchart shown in Figure 4. This flowchart also illustrates the order of destructive crack verification procedures.

3.2.1 Liquid Penetrant Inspection (LPI)

The liquid penetrant inspection was carried out at both AMDU and Orenda by experienced technicians certified at Level II in LPI using the military standard MIL-STD-6866 procedures as described below.

Discs were precleaned by vapour degreasing followed by a solvent rinse. The discs were then dipped into the penetrant bath. Magnaflux ARDROX 985-P2-E penetrant was employed by AMDU using 45 and 60 minutes soaking periods. Orenda employed Magnaflux ARDROX 985P14 and a 30 minute soaking period. The discs were removed from the bath and washed by spraying with water at 40°C. Emulsifier was then applied for two minutes using ARDROX PR4 (AMDU) or ARDROX 9PR12 (ORENDA). The discs were washed again by water spray at 40°C, and checked for proper background with ultraviolet light (black light) and then air dried for 15 minutes. The developer was used both in the form of a dry powder as well as a nonaqueous spray as described below:

a) At AMDU, discs were put into a cloud chamber full of white powder developer and a shot of air was applied such that the component was completely covered with the powder. Then each disc was taken into a dark room and specific crack areas were developed more precisely using ARDROX 9D6 and the discs were inspected on an individual basis for cracks .

b) At Orenda, discs were sprayed using ARDROX D-499C developer and then inspected.

Inspections were performed under a black light with minimum intensity of 800 microwatts per sq. cm at the part surface where the crack indications appeared fluorescent. From the crack indications, an estimation of the crack lengths at the surfaces were made at AMDU using a digital readout vernier calliper which is considered to be accurate to $\pm$0.02 mm. It is not known what instrument was used by Orenda to measure the crack lengths.

Special notes were given to the two AMDU inspectors which indicated that cracks would most probably occur from the bolt holes toward the center of the disc.

A list was obtained for each disc from both inspectors at AMDU indicating the bolt holes which contained cracks and the measured length. Orenda provided NAE with maps which indicated the position and surface length of each crack detected.

3.2.2 Eddy Current Inspection (ECI)

The eddy current inspection was carried out at AMDU by two technicians who were certified at level I in ECI. A Nortec Reichii I instrument equipped with a rotating probe scanner designed specifically for fastener hole inspection was used. The unit operates at a test frequency of 500 kHz. At this frequency, the maximum penetration depth for eddy current in the disc material is approximately 6 mm(8). A 3/16" diameter reflector type differential probe, wrapped in teflon tape, was employed. The wrapping of the probe in teflon tape decreased the clearance between the probe and the hole to within 0.004 to 0.010 inches which in turn decreased the noise level and increased the sensitivity and repeatability of detection. The probe rotates at a speed of 3000 rpm.

If a crack was present, a sine wave was generated on the screen with an amplitude larger than that generated by the machining marks. The location of a crack was determined by the signal position on the screen between 0 and 360°.

Two different sensitivity levels were used by the eddy current inspectors. The first inspector used a gain setting of 2 whereas the second inspector used a more sensitive gain setting of 5 which led to a larger number of positive indications of smaller cracks. Since no relation could be found between the crack length and the signal amplitude using the above instrument, only an indication that a crack existed was noted for each bolt hole.

3.2.3 Real Time Microfocus X-ray Radiography

The Ridge Inc. Microfocus Integrated X-ray Inspection System (MIXIS) was used by AMDU for the discs. The MIXIS has a relatively high resolution microfocus X-ray tube with a high output. A focal spot size as small as 10 microns and magnifications up to 100 times were employed. At 68 kV and 24 mA, the main body of the disc appeared grey, while the thicker outer annulus of the disc appeared darker and the bolt holes much lighter.

The major problem encountered by AMDU when the real time microfocus X-ray technique was applied to the fifth stage compressor discs was the poor contrast between the crack and the surrounding material. At the time of this work, the MIXIS facility at AMDU was not fully equipped with all the necessary peripherals to detect very small cracks. In practice, only cracks longer than 5 mm were detected with confidence. Since a 5 mm detection limit was worse than for the LPI and ECI methods, the inspectors decided to exclude this method from the study.

3.2.4 Ultrasonic Leaky Wave Using a C-scan System

The ultrasonic leaky wave (ULW) technique has been described in detail in Reference 9. This method is not a conventional NDI technique for crack detection in engine components but it was felt that the technique could have potential for such applications. Hence this method was used on an exploratory basis. The procedures employed and the results obtained using the leaky wave technique on compressor discs are unique to this investigation and therefore are described in greater detail in the following paragraphs.

The ultrasonic leaky wave technique is based on the transmission of sound waves from a liquid medium (usually water) onto the surface of the test component at an angle given by the expression:

$$\theta_R = \arcsin \frac{V_1}{V_2} \qquad (5)$$

where V_1, and V_2 are the sound velocities in the liquid medium and the test material respectively. At angle θ_R, the compressional waves travelling in the liquid are mode converted into surface waves in the test medium. The energy of surface waves scattered by surface connected cracks is leaked back into the water and is picked up by a transducer and presented on the CRT or recorded on a chart recorder. The inspection can be performed automatically using a C-scan system which produces a spatial image of defects showing the location and extent of flaws. Figure 5 illustrates a schematic of the test configuration and a CRT presentation from the ultrasonic leaky wave technique used. The most time consuming part of the ULW inspection process is setting up the scanning parameters such as probe angle, thresholds, etc. Once this is accomplished on one disc,

the other discs can be inspected simply by replacing the inspected disc with a new one and repeating the inspection process which usually takes less than 10 minutes.

For inspection of compressor discs, the disc was mounted on a turntable immersed in a water tank. A 10 MHz, one inch focal length probe was positioned at about 20° angle to the disc in order to send and receive ultrasonic waves. Based on a calibration procedure carried out before inspection, this frequency and incident angle was found to result in an optimal signal to noise ratio for the compressor disc investigation. The disc was then automatically rotated while the probe was indexed radially towards the bore after each revolution until the required area of the disc was covered.

The ULW inspection was performed once on each side of the discs by two students from Carleton University after approximately one month of training on the technique and the instruments. The students did not have any formal training in NDI disciplines. The inspection results were independently interpreted by the same individuals.

3.3 Destructive Crack Verification Procedures

In order to determine the reliability of the NDI techniques, all bolt holes from the ten discs were examined and the actual locations and size of the cracks were determined using the procedures described below.

A 1 x 1.5 inch area surrounding each bolt hole was cut out. The bolt holes, where crack indications were identified by the ULW technique, were pried open allowing the crack size to be measured with the aid of a scanning electron microscope (SEM). The remaining bolt holes were cold mounted, polished and examined using an optical microscope. If a crack was observed, it was pried open and the fracture surfaces were examined with the SEM. If no crack could be seen, the bolt hole mounts were broken open and re-mounted on the other side, polished and once again inspected using an optical microscope, and any cracks found were pried open and measured. This procedure was employed in order to reduce the possibility of missing small cracks during pry opening of the bolt holes. Finally, all bolt holes in which no cracks were detected were broken open through the region where cracks normally occurred and if a crack was found, its maximum length as well as the length of the disc surfaces were measured under SEM. This procedure is given in flowchart form in Figure 4.

4.0 RESULTS

4.1 Histograms

The nondestructive and destructive inspection data for all ten compressor discs are provided in a separate report[10]. Since the experimental data from this investigation is of category 2 type (one inspection per crack) the crack lengths had to be grouped into intervals in order to obtain a significant number of cracks to determine realistic POD values. Several crack length intervals between 0.2 mm and 1.0 mm were examined and the best compromise between the number of intervals and the number of cracks in each interval was achieved at an interval of 0.5 mm.

Figures 6 to 11 show histograms of the number of cracks detected, the total number of cracks and the number of cracks missed (ie. total number - detected number) as a function of the crack length interval for each NDI technique. In Table 1, the total and percentage of cracks detected, missed and false calls are presented along with the smallest crack detected and the largest crack missed for each technique.

4.2 Probability of Detection Curves and the 90% POD/95% Confidence Lines

The histograms shown in Figures 6 to 11 were used to obtain the observed POD data points by calculating the ratio of the number of cracks detected in each interval to the total number of cracks in that interval. These points were then used in the linear regression analysis (Equations 1 to 4) to obtain the mean log-logistic POD curves.

The mean POD is subject to statistical variation that result from factors such as the ability and attitude of the operator, the geometry and material of the component and the location, orientation and size of the flaw. Such variations in turn can lead to non-repeatable positive indications for a crack of a particular length[4]. As mentioned earlier, standard statistical methods can be used to obtain confidence limits on the probability of detection data. In order to determine which statistical distribution was best suited to describe this type of data (category 2), a number of distributions were used to calculate the 95% confidence bound on the log-logistic POD curve for the different NDI techniques investigated. The different distributions used in the comparison and the results obtained are described in greater detail in Appendix A. The results indicate that in both the normal and the student t-distributions, as the crack lengths increase the confidence

bounds approach closer to the mean POD line indicating that larger cracks are more likely to be detected. The confidence bound obtained using the normal distribution was slightly closer to the POD curve than the student t-distribution. Other distributions resulted in less realistic confidence limits and, therefore, the normal distribution is used to obtain the 95% confidence bounds for all POD curves.

Figures 12 to 17 illustrate the observed data, a mean log-logistic POD curve fitted to the data and a 95% lower confidence bound obtained by using the normal distribution for each NDI technique. A crack size detectable at 90% POD with 95% confidence level has been suggested by U.S. Air Force MIL-STD-1783 for use as the initial crack length in damage tolerance applications. Hence, it was decided to use the crack size at 90% POD from the 95% confidence bound to compare the different NDI techniques. These initial crack lengths are given in Table 2 for each NDI technique.

4.3 Measured Versus Estimated Crack Lengths

Another aspect of NDI techniques which must be considered is the ability of the techniques to size the cracks accurately. A quantitative measurement was carried out on some of the discs in order to determine the accuracy of different NDI methods in sizing the cracks. Crack lengths along the surfaces of three discs were measured with the aid of a scanning electron microscope and then compared to the crack lengths obtained from the various NDI techniques for which crack length measurements were possible. Orenda's LPI results were not included in this analysis since the crack lengths obtained did not appear to be as accurate as those obtained from the other techniques. Also, the eddy current instrument used in this study did not provide accurate indications of the crack size so that ECI results were not used. The results for the other techniques are shown in Figures 18 to 20. The best fit line through the data was obtained using the least squares method, the results of which are given in Table 3. This table gives the slope, intercept and correlation coefficient for the best fit line for the surface crack lengths and also the maximum crack lengths. The latter will be discussed in more detail in the next chapter.

5.0 DISCUSSION

Of the 400 bolt holes which were examined by optical microscopy and later by SEM, 333 of them contained cracks up to 8.5 mm in length. The best of the LPI techniques shown in Figure 8 resulted in 125 detections (37.5%), 208 misses (62.5%) and 2 false calls

(0.6%). The largest crack missed by the best LPI method was 3.69 mm in length. The detection results for the eddy current inspection technique with a high gain setting (ECI5), Figure 10, were much better than those for the LPI methods. The total number of cracks detected by ECI5 procedure was 253 (76%). However, the number of false calls for this method at 8 (2.4%) was also higher. The largest crack length missed by ECI5 was 2.7 mm and the number of cracks missed was 80 (24%). Assuming that the 2.7 mm crack was missed because of an operator error, then the second largest crack which was missed was 1.27 mm. Although the number of cracks detected by the ULW technique at 167 (50.2%) was not as high as for the ECI5, this technique did detect all cracks larger than 1.5 mm. Also the number of false calls was only 2 (0.6%).

Of the POD curves shown in Figures 12 to 14 for the LPI procedures, the 60 minute dye penetrant soaking period (LPI60) gave the best results of the three. The POD curve for the eddy current technique with a low gain setting (ECI2), shown in Figure 15, gave similar results as compared to the LPI technique with a dye penetrant soaking period of 45 minutes (LPI45) but the crack size detectable at 90% POD with 95% confidence for the ECI2 technique was greater than 10 mm as opposed to 8.35 mm for LPI45. At 4.10 mm, the ECI5 technique gave the best 90/95 limit of all the techniques except for the ULW technique which resulted in a 2.90 mm detectable crack limit at 90% POD/95% confidence. Although the ECI5 technique was the most sensitive for detecting small cracks (less than 1 mm), the ULW technique appears to be the most reliable of all the techniques since it detected all cracks greater than 1.5 mm. It should be emphasized that two inexperienced students were used to inspect the discs using the ULW technique and to interpret the crack maps generated. Since NDI results are generally dependent on operator skill and experience, one would expect that the POD results for the ULW method would improve further if experienced technicians were to perform the inspections.

If the 2.7 mm crack missed by the ECI5 technique could be attributed to operator error and considered detected, then the resulting POD curve, shown in Figure 21 would give a 90/95 limit of 1.75 mm. This in turn would change the outcome of our study by showing that the manual ECI5 technique was the most sensitive and reliable of all the NDI techniques examined followed by the ULW technique.

As already mentioned, the 90% POD at 95% confidence limit was established for damage tolerance applications for aircraft airframe structures where most of the critical components are not readily accessible. Since a gas turbine engine must be disassembled in

order to inspect the different components, each component can be inspected as many times as is deemed necessary. Therefore, it has been suggested that the intercept point of the 90% POD with the mean POD line may be a more realistic criterion for choosing the best NDI technique for implementing the damage tolerance based maintenance methodologies for engine components. These limiting crack lengths are given in Table 4 and show that the ECI5 technique results in the smallest crack length of 1.65 mm (1.25 mm if the 2.7 mm missed crack is ignored) followed by the ULW technique with a value of 1.85 mm.

In terms of the crack sizing ability of NDI techniques, the ULW technique appears to result in the best correlation between the estimated crack length and the measured length along the surface of the disc as determined by scanning electron microscopy. As seen in Table 3, the slope of the mean line and the correlation coefficient for this technique was 0.93 and 0.73, respectively as compared to 0.78 and 0.88 for the LPI technique with a soaking period of 60 minutes. When the estimated crack lengths are compared to the maximum crack length (also determined by scanning electron microscopy), the slope and correlation coefficient was 0.99 and 0.92 as shown in Figure 22 and compared to the LPI techniques in Table 3. This indicates that the crack lengths determined from the ULW technique are chosen approximations to the maximum crack length rather than the crack length along the surface of the disc. This can be an important factor if crack curvature or tunneling is significant in a given component. This effect is due to the fact that ultrasonic leaky waves penetrate about 1.5 times the wavelength (ratio of sound velocity to the frequency which is approximately 0.3 mm for steel at 10 MHZ) into the material, interacting with the surface area of a crack. On a number of occasions during this investigation, the ULW method picked up cracks beneath the disc surfaces.

6.0 CONCLUSIONS

The sensitivity and reliability of several NDI techniques in the detection and sizing of low cycle fatigue cracks in the tie bolt holes of fifth stage compressor discs of J85-CAN40 engines have been assessed. In this assessment, the conventional liquid penetrant and manual eddy current techniques have been used along with newer microfocus X-ray and ultrasonic leaky wave techniques to inspect ten retired compressor discs which contained cracks. The following observations have been made:

1. The microfocus X-radiography failed to detect small cracks due to technical difficulties associated with the operation of the system at the time of this investigation and thus was excluded.

2. The liquid penetrant inspection techniques varied greatly depending on the dye penetrant soaking period employed. The best of the LPI techniques (LPI60) resulted in 37.5% detections, 62.5% misses and 0.6% false calls. The largest crack missed by the LPI technique was a 3.7 mm crack. The crack length at 90% POD on the mean log-logistic curve was 3.45 mm and on the 95% confidence bound using the normal distribution was 6.2 mm. The LPI technique provided an estimate of the crack size, though the technique tends to underestimate the crack length. A correlation factor of 0.84 was found between the crack length along the surfaces and the LPI results by fitting a straight line through the data points using the least squares method. The correlation factor between the maximum crack length and the LPI results was 0.86. The dye penetrant soaking period has a significant effect on the number of cracks detected by the liquid penetrant technique since only 27.9% of the cracks were detected by the 30 minute soaking period as compared to 37.5% for 60 minute soaking time.

3. The manual eddy current technique at a high sensitivity level detected a larger number of cracks (76% detections, 24% misses). However the rate of false calls (2.4%) and the largest crack missed (2.7 mm) were relatively high. The crack lengths at 90% POD/mean and 90% POD/95% confidence were 1.65 and 4.1 mm, respectively. If this 2.7 mm crack length missed was due to operator error and not the fault of the technique and therefore considered detected, the 90%/mean and 90/95 POD limits become 1.25 and 1.75 mm, respectively. In terms of the capability of detecting small cracks (sensitivity), this technique was superior to all other methods examined in this investigation. It should be strongly emphasized that a manual eddy current technique was used in this investigation. This means that the probe placement was accomplished by hand which should have a strong influence on the reliability and sensitivity of the technique.

4. In terms of reliability, the ultrasonic leaky wave technique using an automated C-scan system produced the most impressive detection results for cracks larger than 1.5 mm (100% detection). For smaller cracks however, the detection rate was not as good as that for the high gain eddy current method. This technique had 50.2%

detections, 49.8% misses and 0.6% false calls. These results may be improved by using a more sensitive high frequency transducer, smaller index and full amplitude measurement. Another advantage of the leaky wave method is its capability of crack size estimation. A good correlation factor of 0.92 was found between the crack length estimated by the ULW method and the maximum crack length as measured by SEM.

7.0 ACKNOWLEDGEMENTS

The authors wish to thank Major R.A. Raoux, Major R. Drummond, Captain D. Masters, Mr. J. McCanna and Mr. J. Stewart of the Aircraft Maintenance Development Unit for their valuable cooperation during the course of this project. The personnel at Orenda Division of Hawker Siddley Canada Inc. were also very helpful and provided the ten service-exposed fifth stage compressor discs which made this programme possible. Mr. M.L. Edkins helped in cutting the specimens and Mr. R.V. Dainty, Mr. D. Chow and Mr. D.D. Morphy assisted with the specimen preparation and SEM. The authors gratefully acknowledge the constant encouragement of Dr. W. Wallace of NAE in completing the programme and preparation of this report.

8.0 REFERENCES

1. Harris, J.A. Jr, Simms, D.L. and Annis, C.G. Jr, 'Concept Definition: Retirement for Cause of F100 Rotor Components', AFWAL-TR-80-4118, 1980.

2. Hill, R.L., Reismann, W.H. and Ogg, J.S., 'A Retirmenet-for-Cause Study of an Engine Turbine Disk', AFWAL-TR-81-2094, November 1981.

3. Satter, S.A. and Sundt, C.V., 'Gas Turbine Engine Disk Cyclic Life Prediction', J. Aircraft, Vol. 12, No. 4, April 1975, pp. 360-365.

4. Berens, A.P. and Hovey, P.W., 'Statistical Methods for Estimating Crack Detection Probabilities', Probabilistic Fracture Mechanics and Fatigue Methods: Applications for Structural Design and Maintenance, ASTM STP 798, 1983.

5. Lewis, W.H., Dodd, B.D., Sproat, W.H. and Hamilton, J.M., 'Reliability of Nondestructive Inspections', July 1974 to December 1978, Final Report No. SA-ALC-MEE 76-6-38-1, US Air Force, Performing Organization Lockheed-Georgia Co., Controlling Office, San Antonia Air Logistics Center, Kelly Air Force Base, Texas, 1978.

6. Yee, B.G.W., Chang, F.H., Couchman, J.C., Lemon, G.H. and Packman, P.F., 'Assessment of NDE Reliability Data', General Dynamics, Fort Worth, Texas, July 1974 - September 1976, NASA-CR-134991, Final Report, October 1976.

7. Koul, A.K., Thamburaj, R., Wallace, W., Raizenne, M.D. and de Malherbe, M.C., 'Practical Experience with Damage Tolerance Based Life Extension Concepts for Turbine Engine Components', Proc. AGARD-SMP Conference on Damage Tolerance Concepts for Critical Engine Components, AGARD-CP-293, San Antonio, Texas, 1985, pp. 23-1 to 23-22.

8. Nortec RECHII I, Rotating Eddy Current Hole Inspection Instrument, Operating Manual, 1981, Revised 1982.

9. Fahr, A., Bellinger, N.C. Stoute, P. and Koul, A.K., 'Inspection of Compressor Discs by Ultrasonic Leaky Waves Using an Automated C-scan System', NRC, NAE LTR to be published.

10. Bellinger, N.C., Stoute, P., Gould, G., Fahr, A. and Koul, A.K., 'The Nondestructive and Destructive Inspection Data for J85-CAN40 Compressor Discs for Detecting LCF Bolt Hole Cracks', NRCC, NAE ST-490, 5 January 1988.

11. Ang, A. and Tang, W.H., 'Probability Concepts in Engineering Planning and Design', Volume 1 Basic Principles, John Wiley and Sons Inc., New York, 1975.

12. Natrella, M.G., 'Experimental Statistics', U.S. National Bureau of Standards, Handbook 91, U.S. Government Printing Office, 1966.

TABLE 1: Summary of Results for NDI Techniques

NDI Technique	No. of Cracks Detected Total	%	No. of Cracks Missed Total	%	No. of False Calls Total	%	Smallest Crack Detected (mm)	Largest Crack Missed (mm)
Ultrasonic Leaky Waves	167	50.2	166	49.8	2	0.6	0.17	1.48
Eddy Current 2	137	41.1	196	58.9	3	0.9	0.23	4.43
Eddy Current 5	253	76	80	24	8	2.4	0.09	2.7 (1.7)*
LPI (45 min)	99	29.7	234	70.3	0	0	0.2	4.33
LPI (60 min)	125	37.5	208	62.5	2	0.6	0.55	3.70
LPI (30 min)	93	27.9	240	72.1	3	0.9	0.5	3.98

* If the 2.7 mm crack is assumed to be detected by the operator

TABLE 2: Intercepts of the 90% POD at 95% Confidence Using Normal Distribution

NDI Technique	90% POD/95% Confidence Limit
Ultrasonic Leaky Waves	2.90
Eddy Current 2	10
Eddy Current 5	4.10 (1.75)*
LPI (45 min)	8.35
LPI (60 min)	6.20
LPI (30 min)	6.40

* If the 2.7 mm crack is assumed to be detected by the operator

TABLE 3: Slope, Intercept, and Correlation Coefficient (R^2) for Surface Indicated Cracks and Maximum Crack Lengths

NDI Technique	Actual Crack Length Along Surface vs NDI Estimated Crack Length			Maximum Crack Length vs NDI Estimated Crack Length		
	Slope	Intercept	R^2	Slope	Intercept	R^2
Ultrasonic Leaky Waves	0.93	0.02	0.73	0.99	-0.2	0.92
LPI (45 min)	0.86	-0.68	0.86	0.76	-1.22	0.85
LPI (60 min)	0.78	-0.60	0.88	0.82	-0.66	0.92

TABLE 4: Intercepts of the 90% POD and Log-Logistic Mean POD Line

NDI Technique	90% POD/Mean Line
Ultrasonic Leaky Waves	1.85
Eddy Current 2	5.60
Eddy Current 5	1.65 (1.25)*
LPI (45 min)	4.25
LPI (60 min)	3.45
LPI (30 min)	3.75

* If the 2.7 mm crack is assumed to be detected by the operator

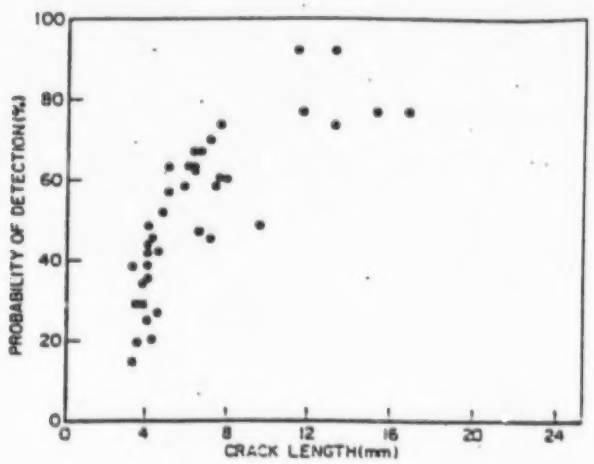

Figure 1: Probability of detection for category 3 type data -60 inspections per crack[4]

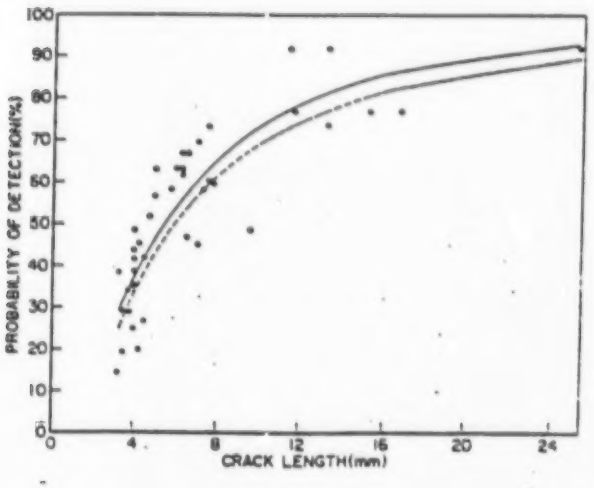

Figure 2: Log-logistic probabiltiy of detection curve with a 95% confidence bound[4]

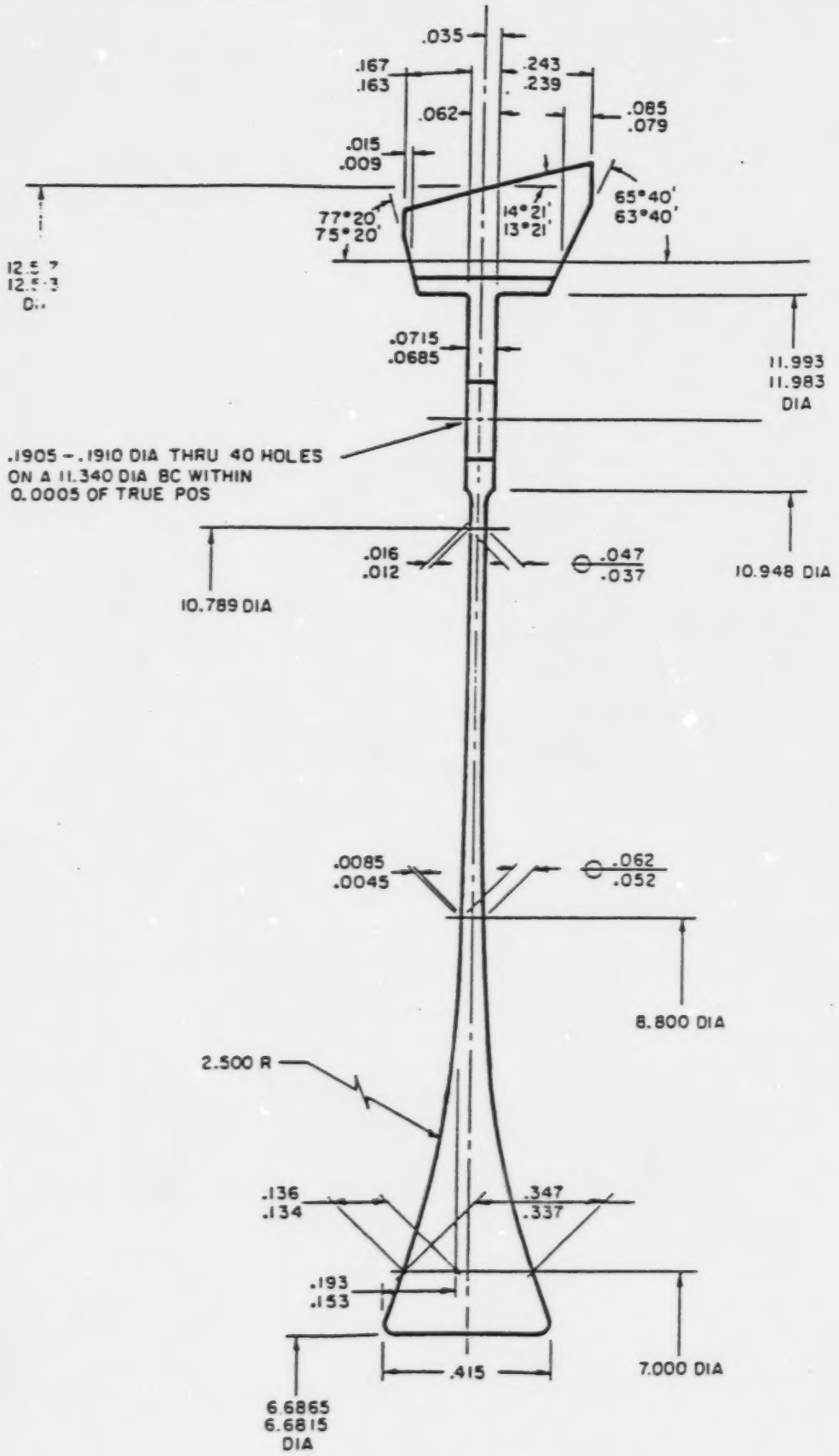

Figure 3: Fifth stage J85-CAN40 compressor disc cross section

Figure 4: NDI and Fractography Flowchart

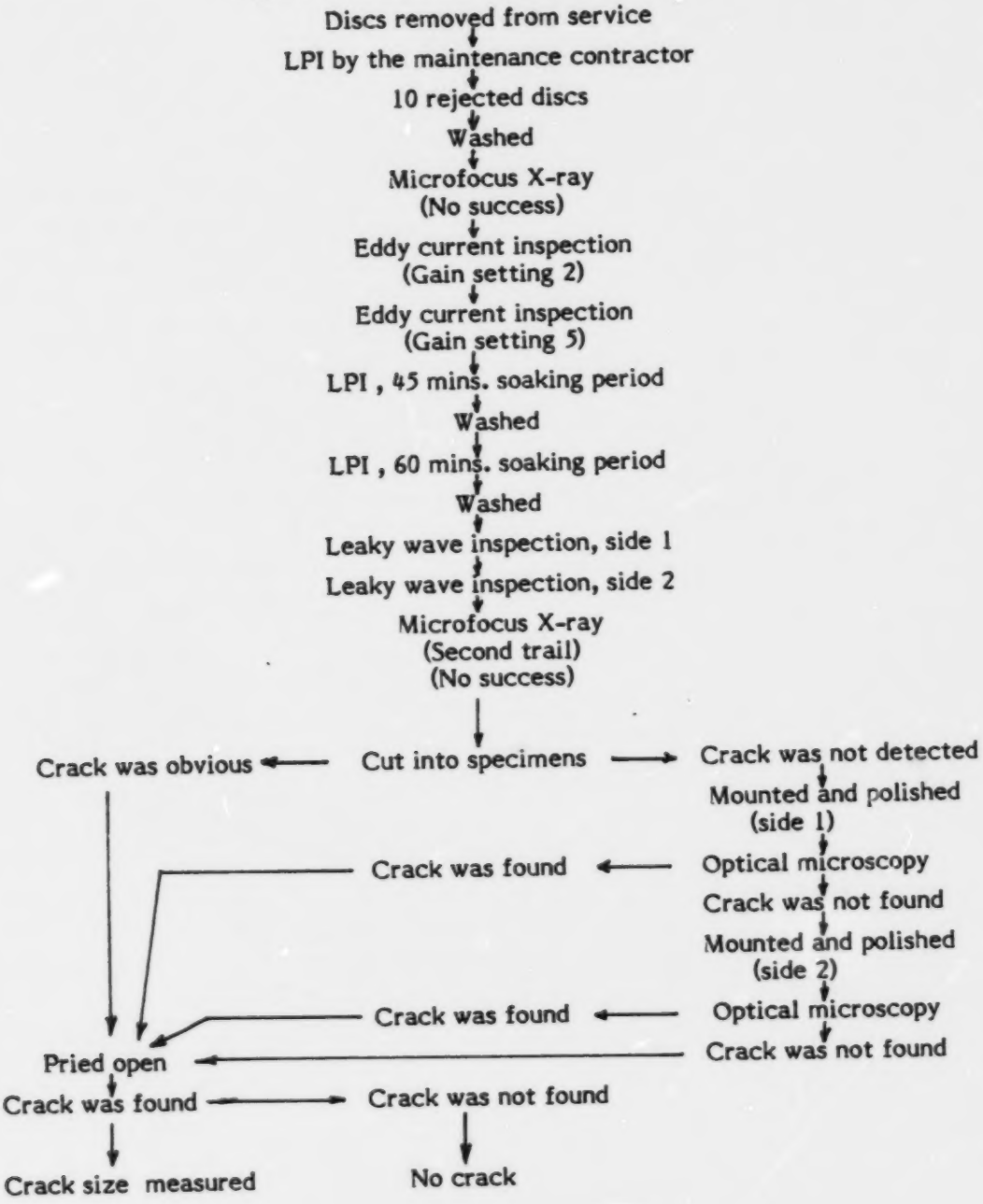

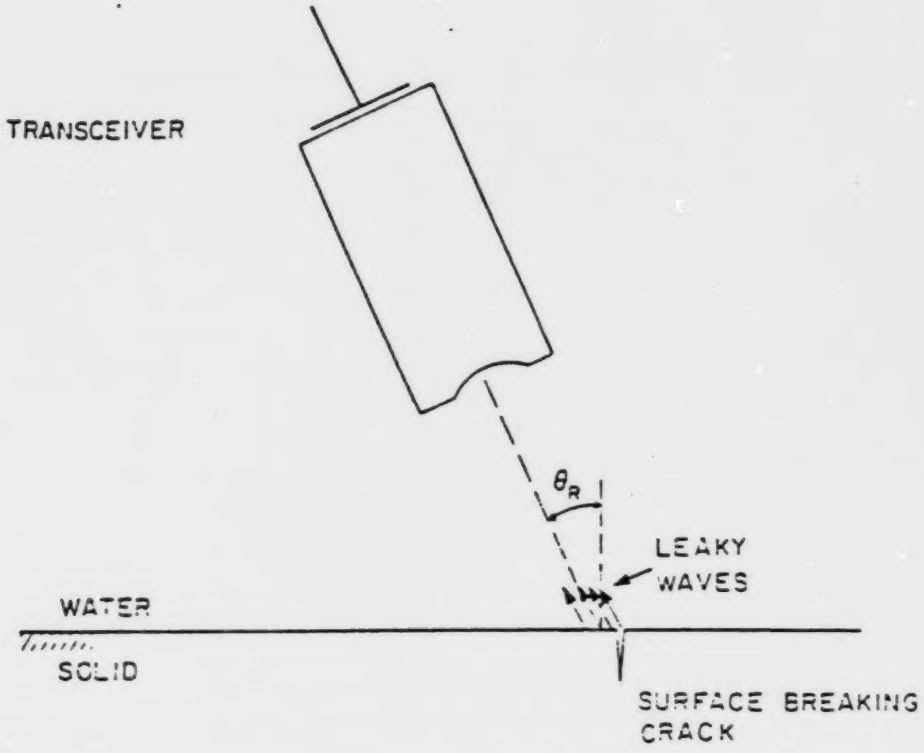

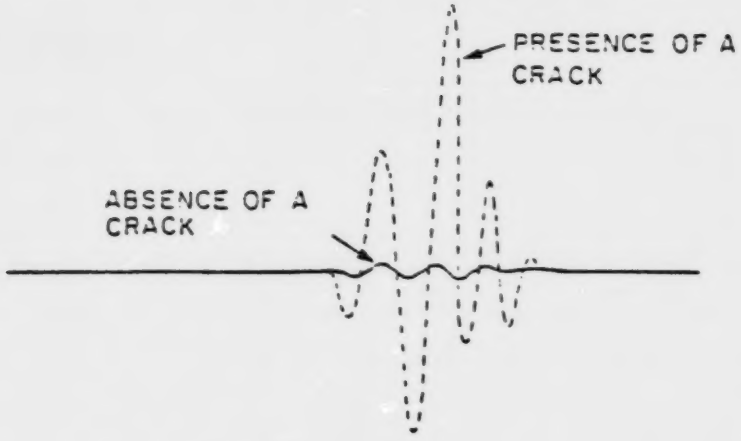

Figure 5: ***ULW test configuration and a typical CRT presentation at the absence and the presence of a crack***

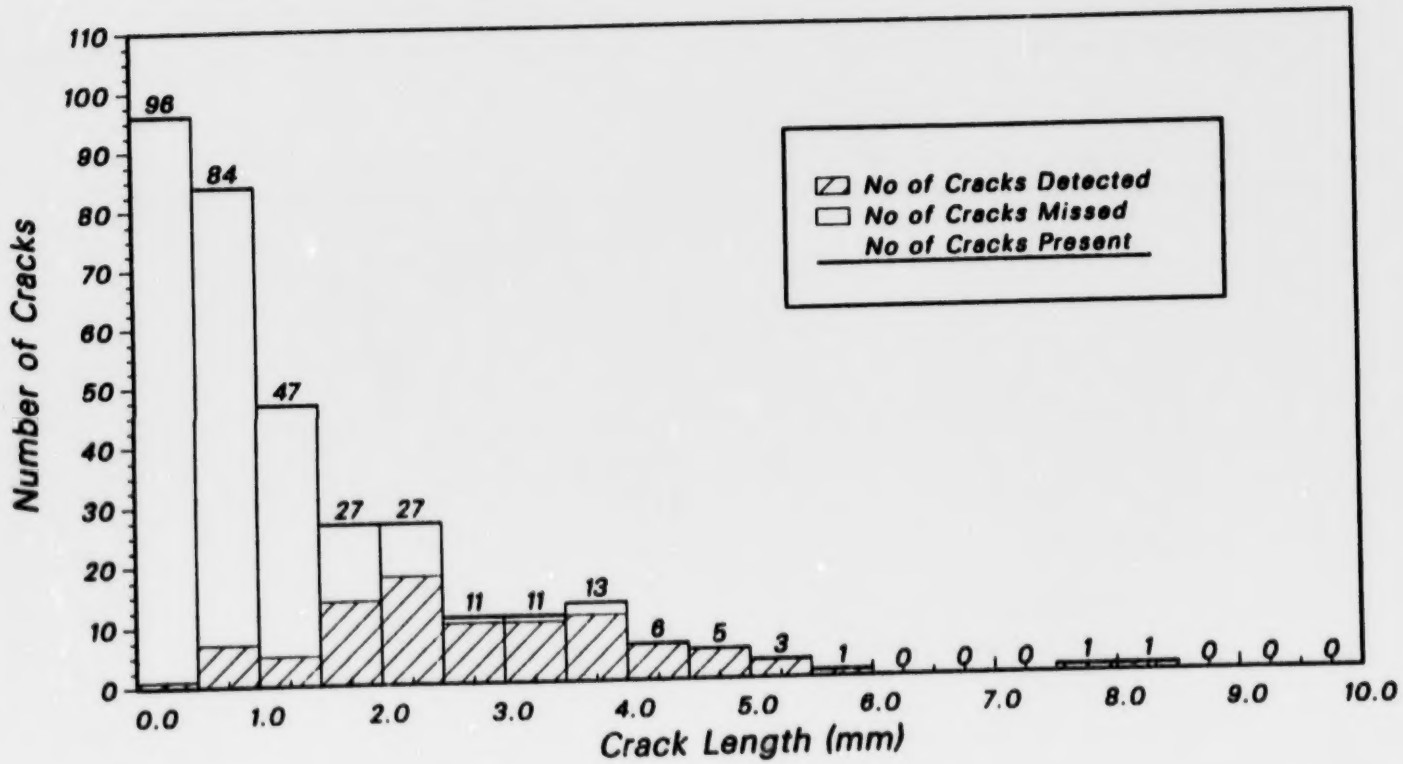

Figure 6: *Histogram showing the number of cracks detected, missed and present as a function of crack length interval for the liquid penetrant inspection technique using a 30 minute dye penetrant soaking period (carried out by ORENDA)*

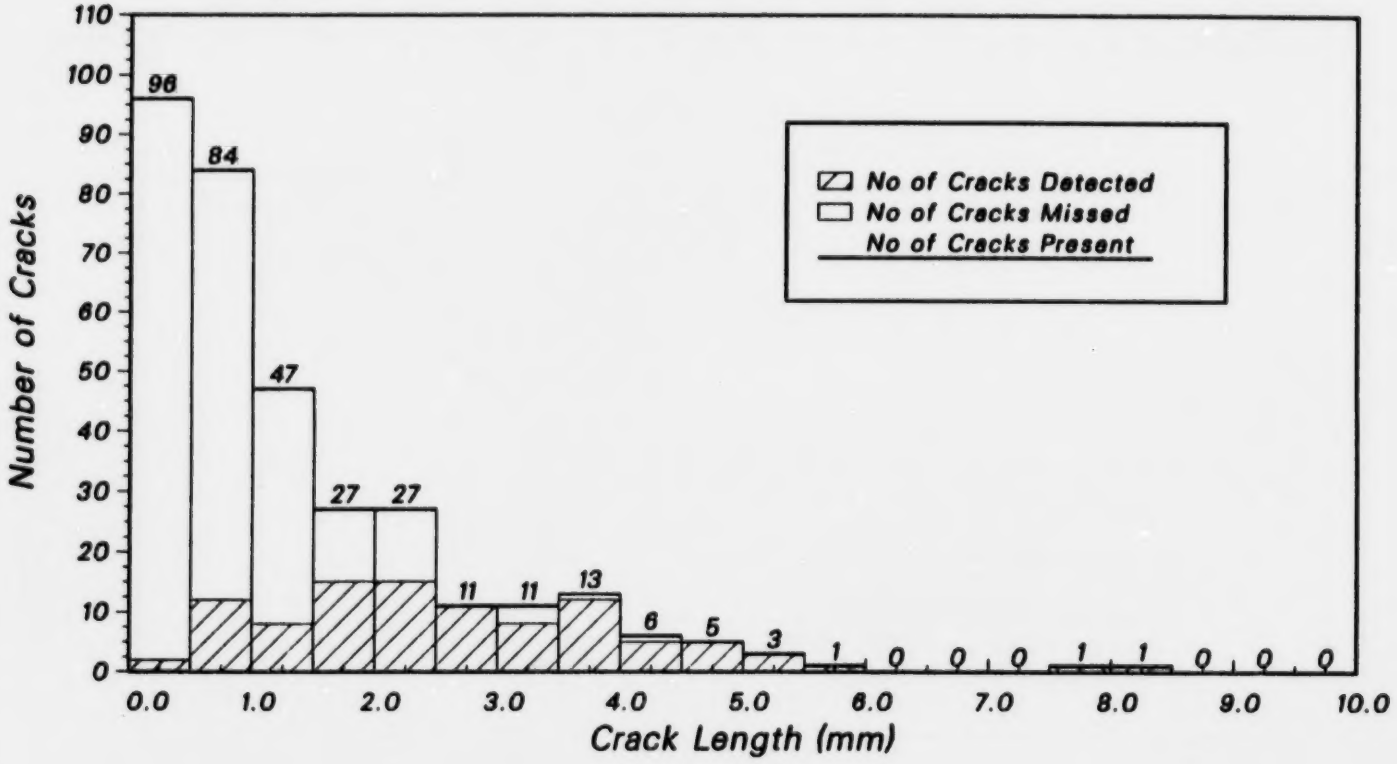

Figure 7: Histogram showing the number of cracks detected, missed and present as a function of crack length interval for the liquid penetrant inspection technique using a 45 minute dye penetrant soaking period (carried out by AMDU)

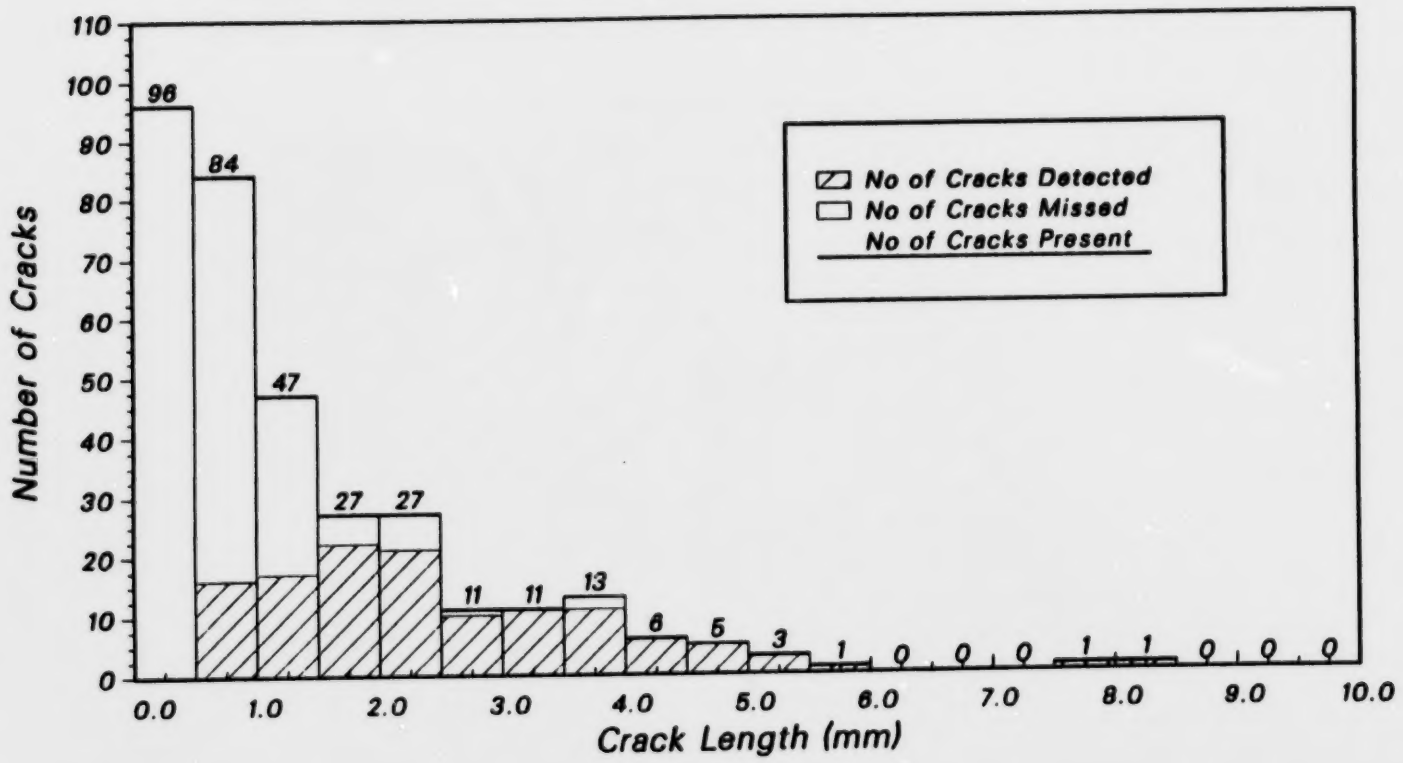

Figure 8: *Histogram showing the number of cracks detected, missed and present as a function of crack length interval for the liquid penetrant inspection technique using a 60 minute dye penetrant soaking period (carried out by AMDU)*

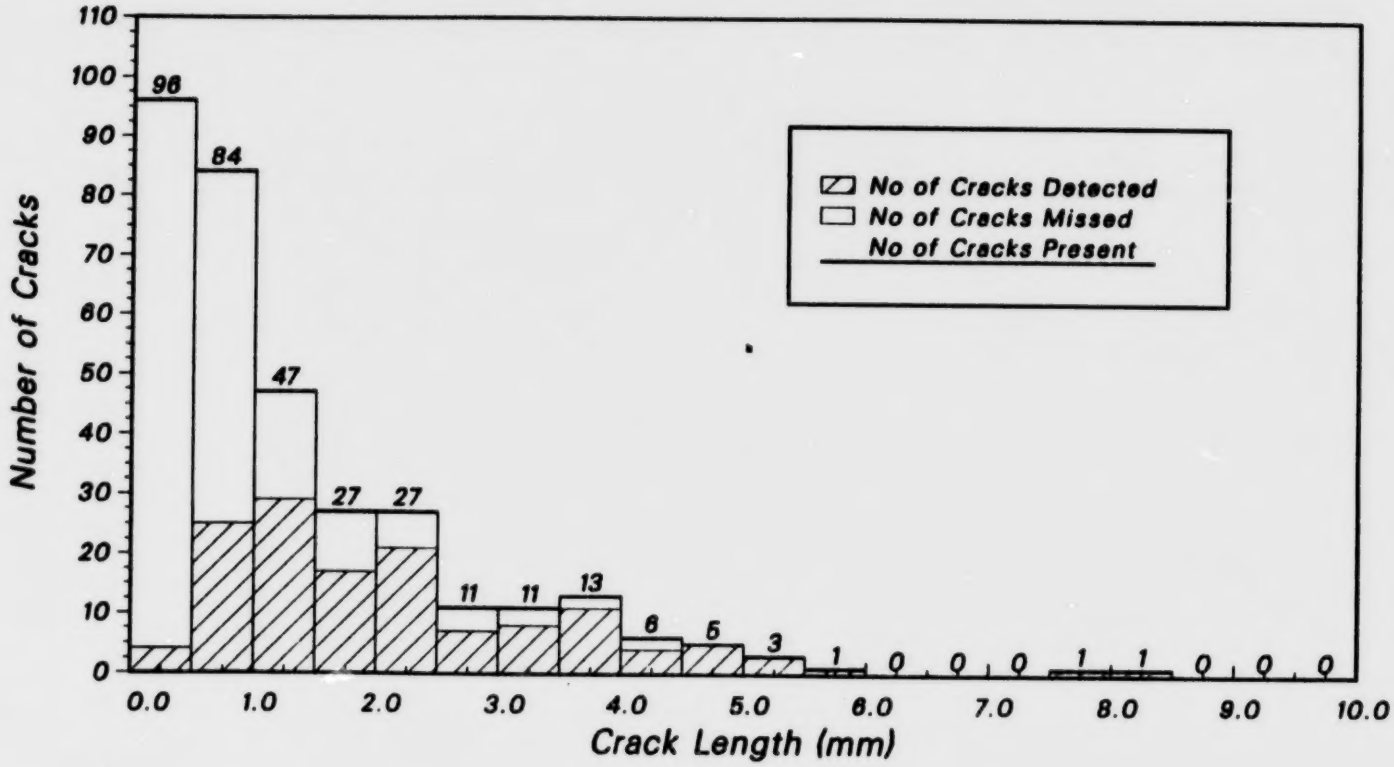

Figure 9: Histogram showing the number of cracks detected, missed and present as a function of crack length interval for the manual eddy current technique at a low gain setting (carried out at AMDU)

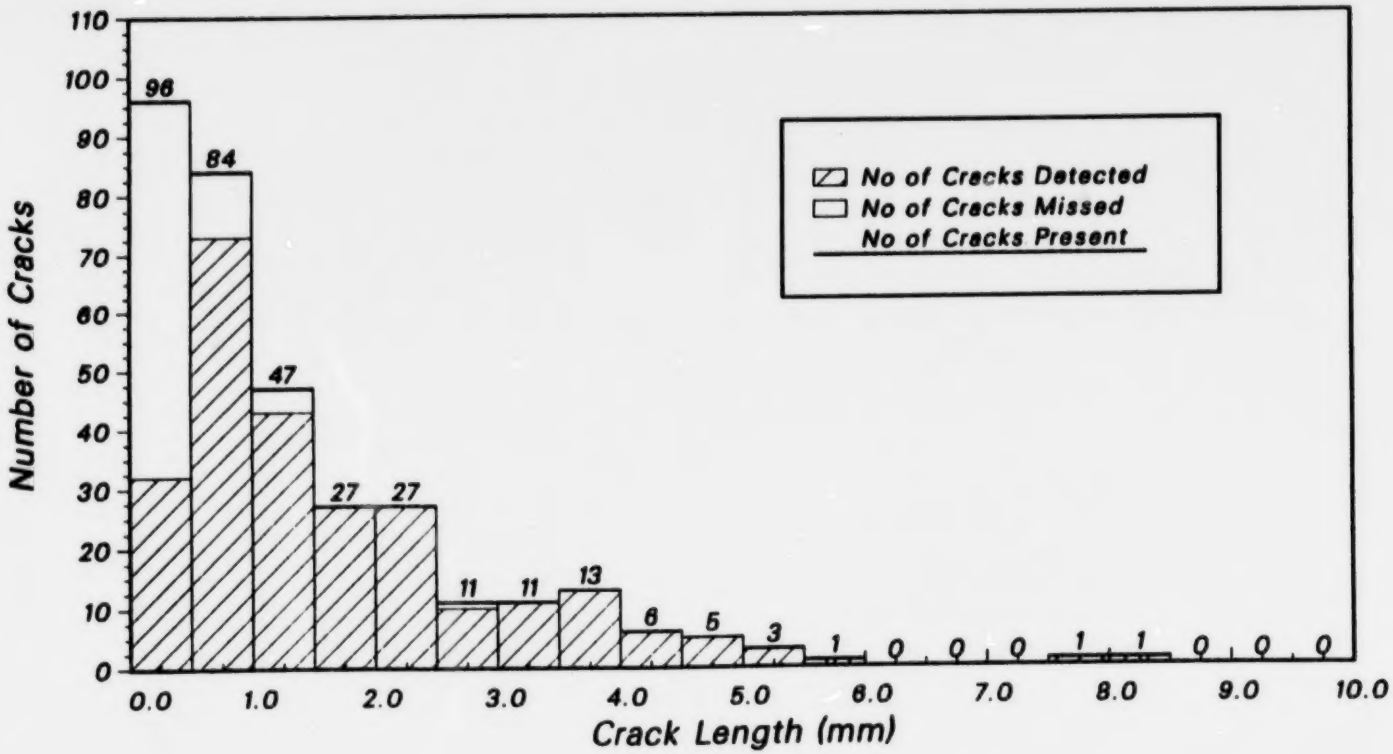

Figure 10: Histogram showing the number of cracks detected, missed and present as a function of crack length interval for the manual eddy current technique at a high gain setting (carried out by AMDU)

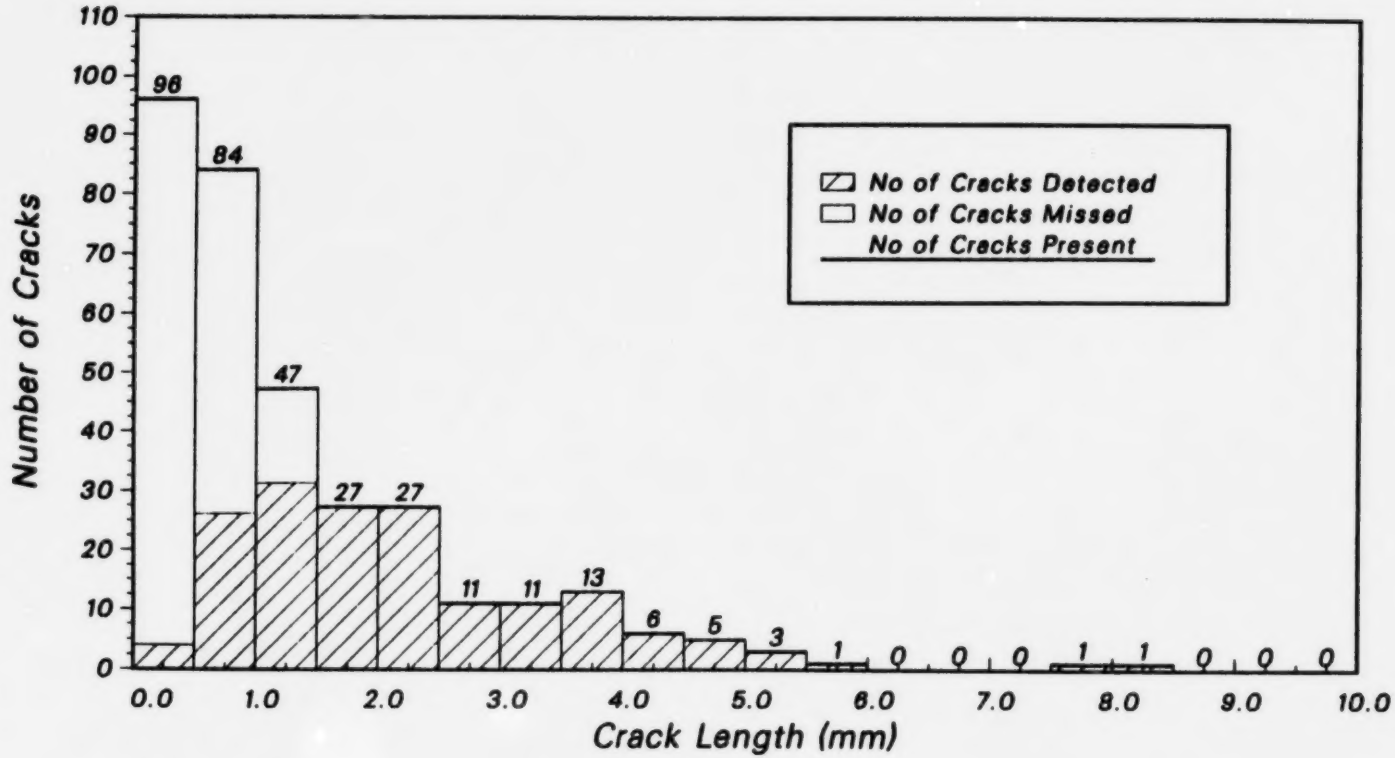

Figure 11: Histogram showing the number of cracks detected, missed and present as a function of crack length interval for the ultrasonic leaky wave technique (carried out by NAE)

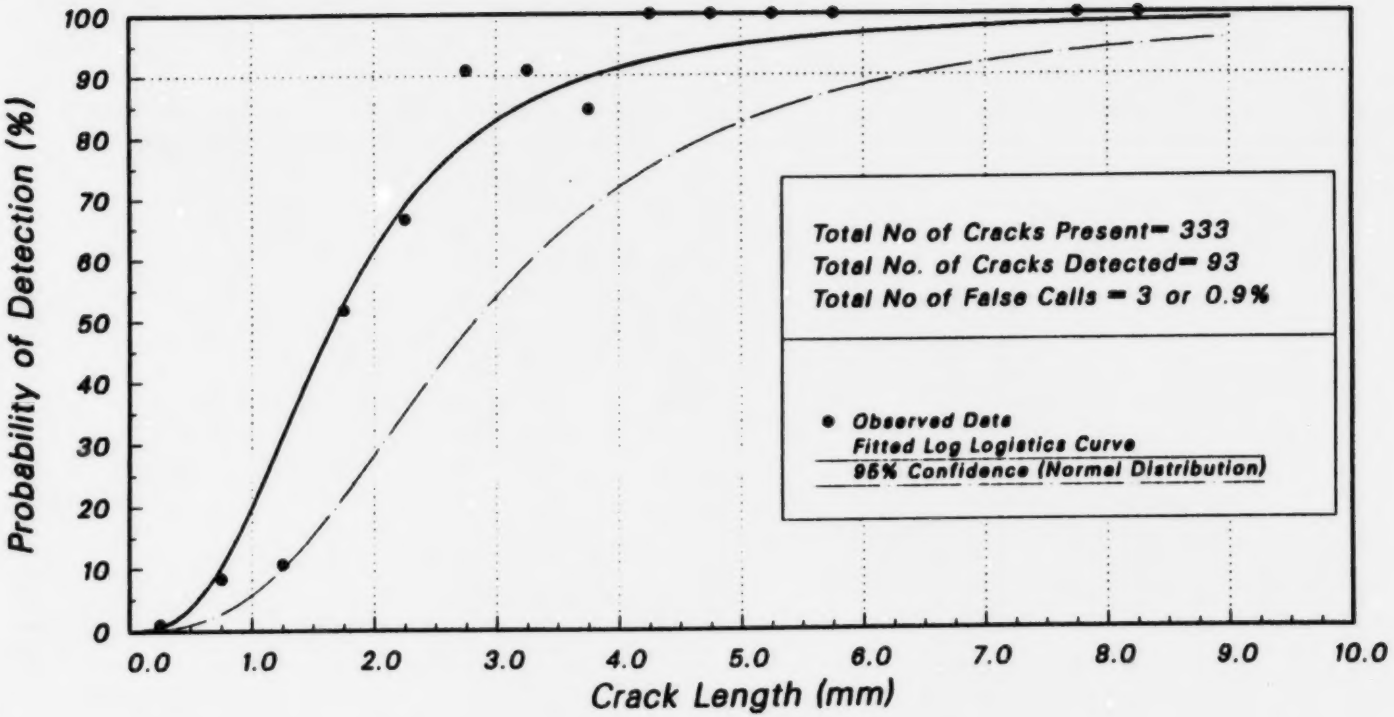

Figure 12: Probability of detection of LCF cracks in compressor discs using liquid penetrant inspection. ORENDA results, 30 minute dye soaking period

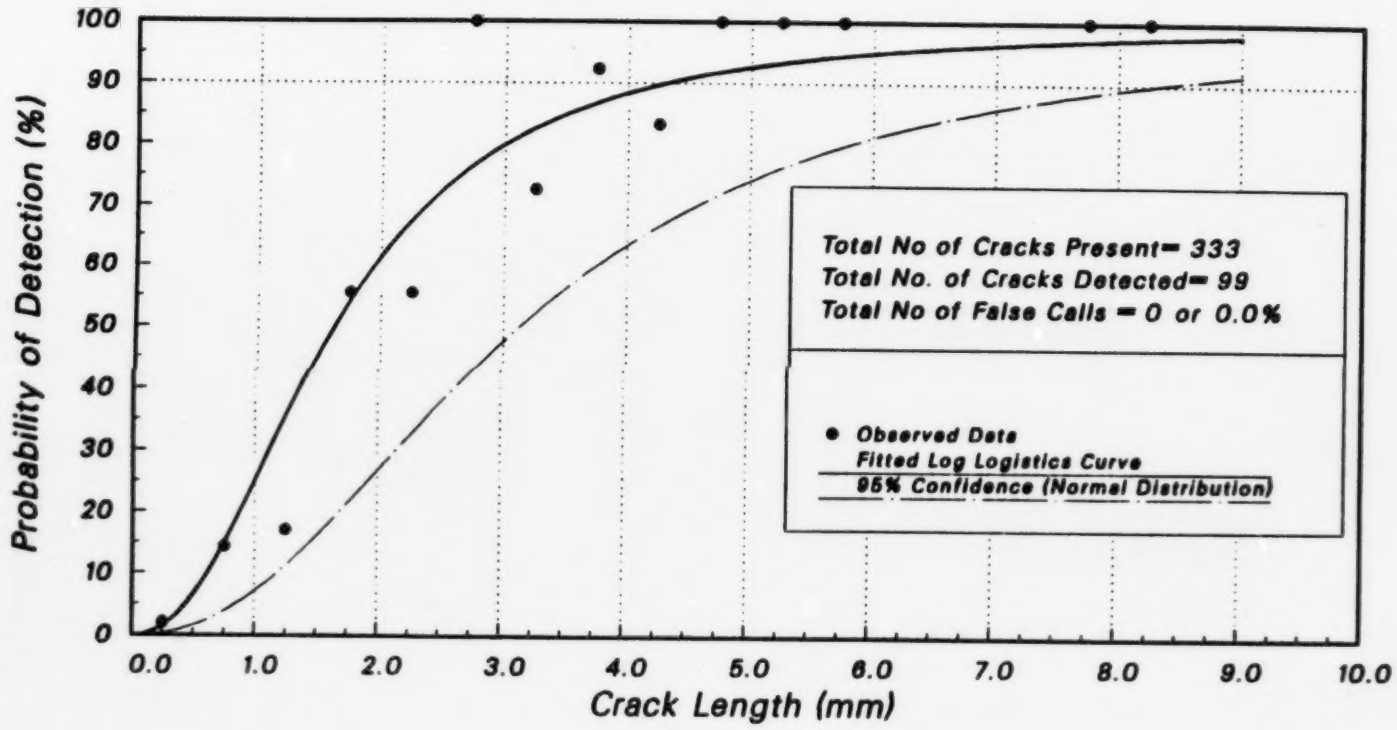

Figure 13: Probability of detection of LCF cracks in compressor discs using liquid penetrant inspection. AMDU results, 45 minute dye soaking period

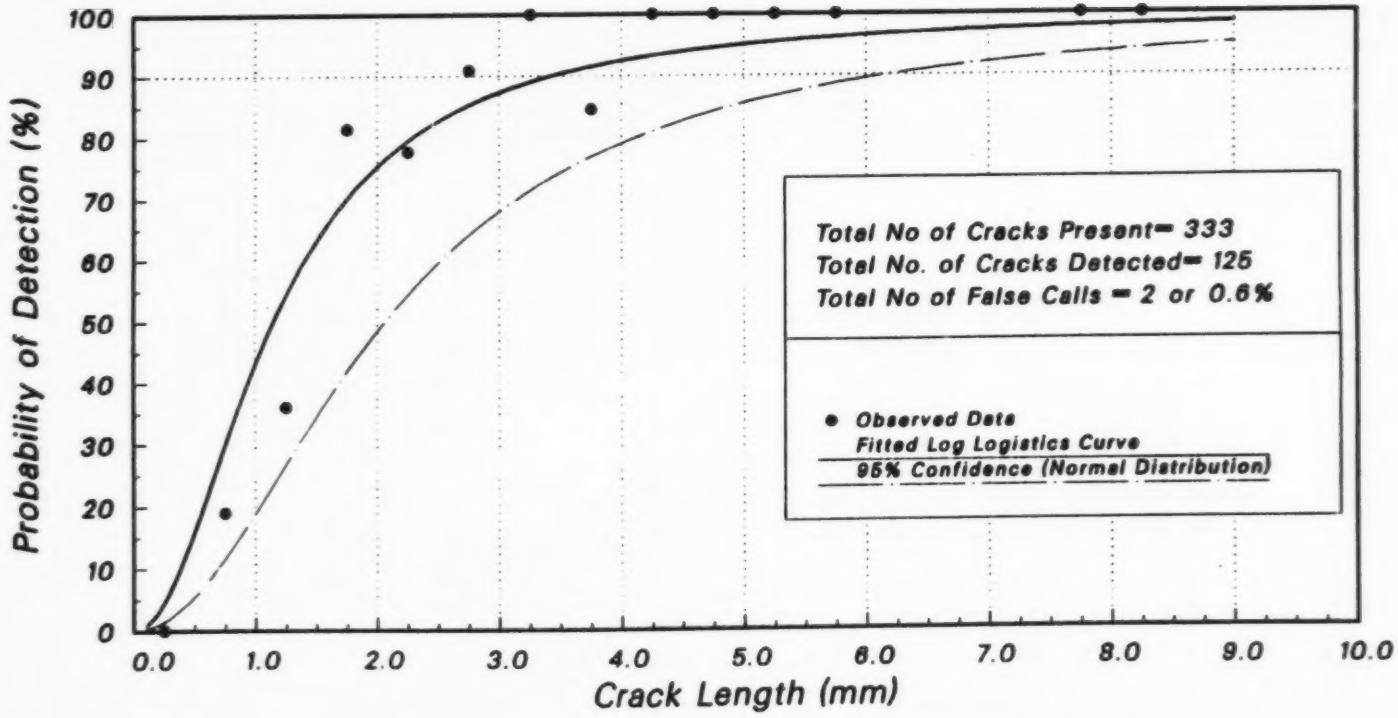

Figure 14: Probability of detection of LCF cracks in compressor discs using liquid penetrant inspection. AMDU results, 60 minute dye soaking period

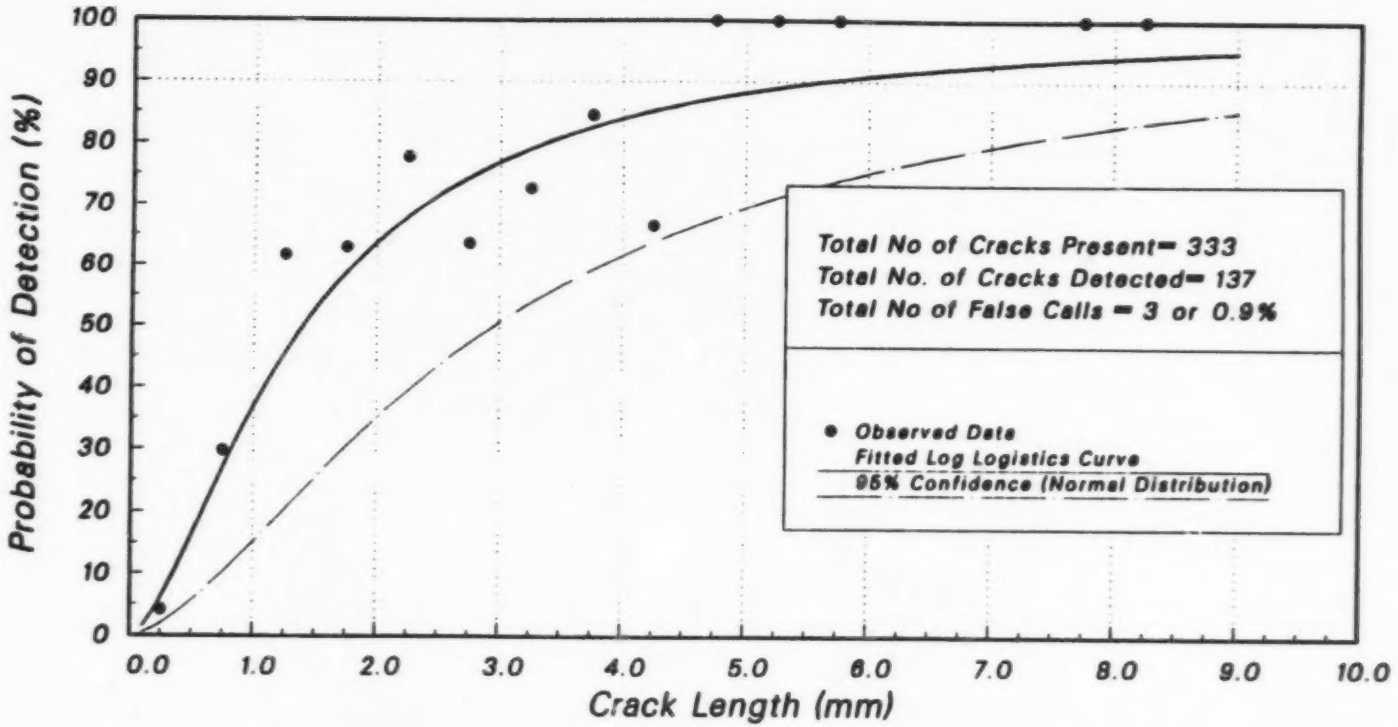

Figure 15: Probability of detection of LCF cracks in compressor discs using manual eddy current technique. AMDU results, low gain setting

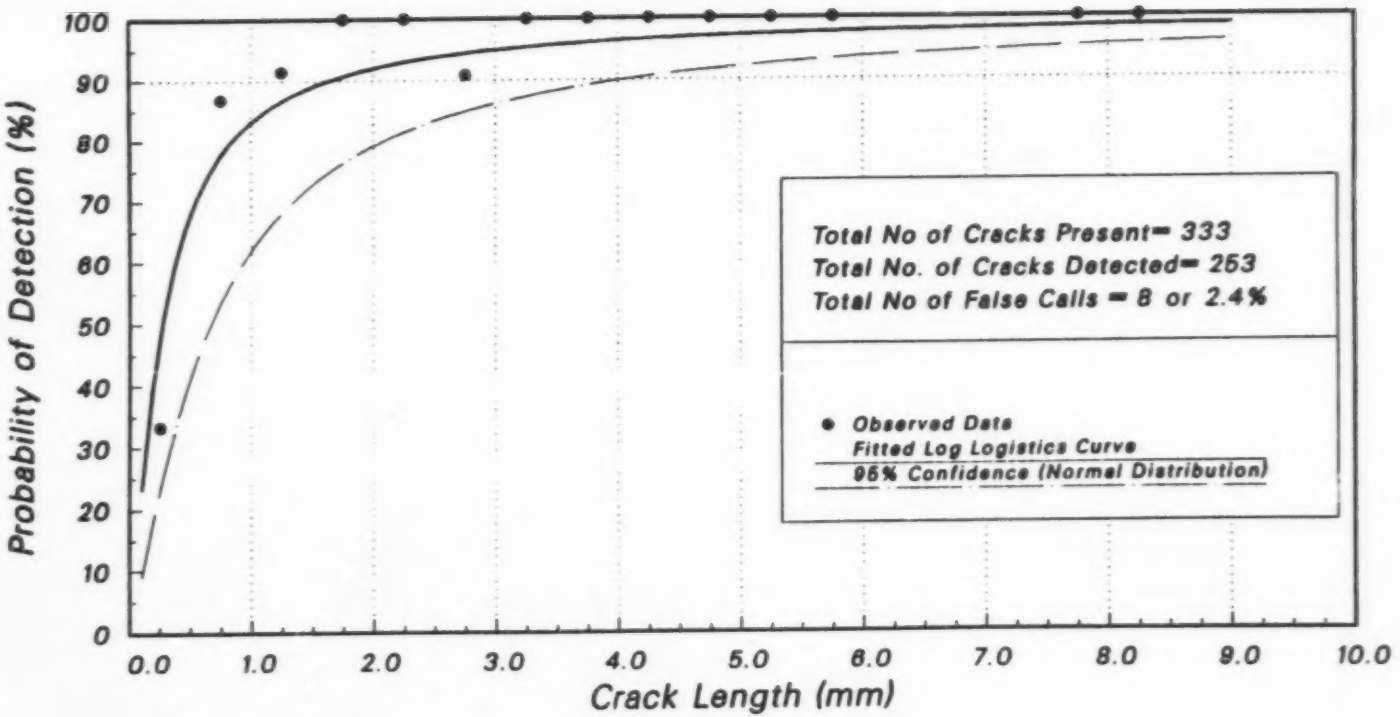

Figure 16: Probability of detection of LCF cracks in compressor discs using manual eddy current technique. AMDU results, high gain setting

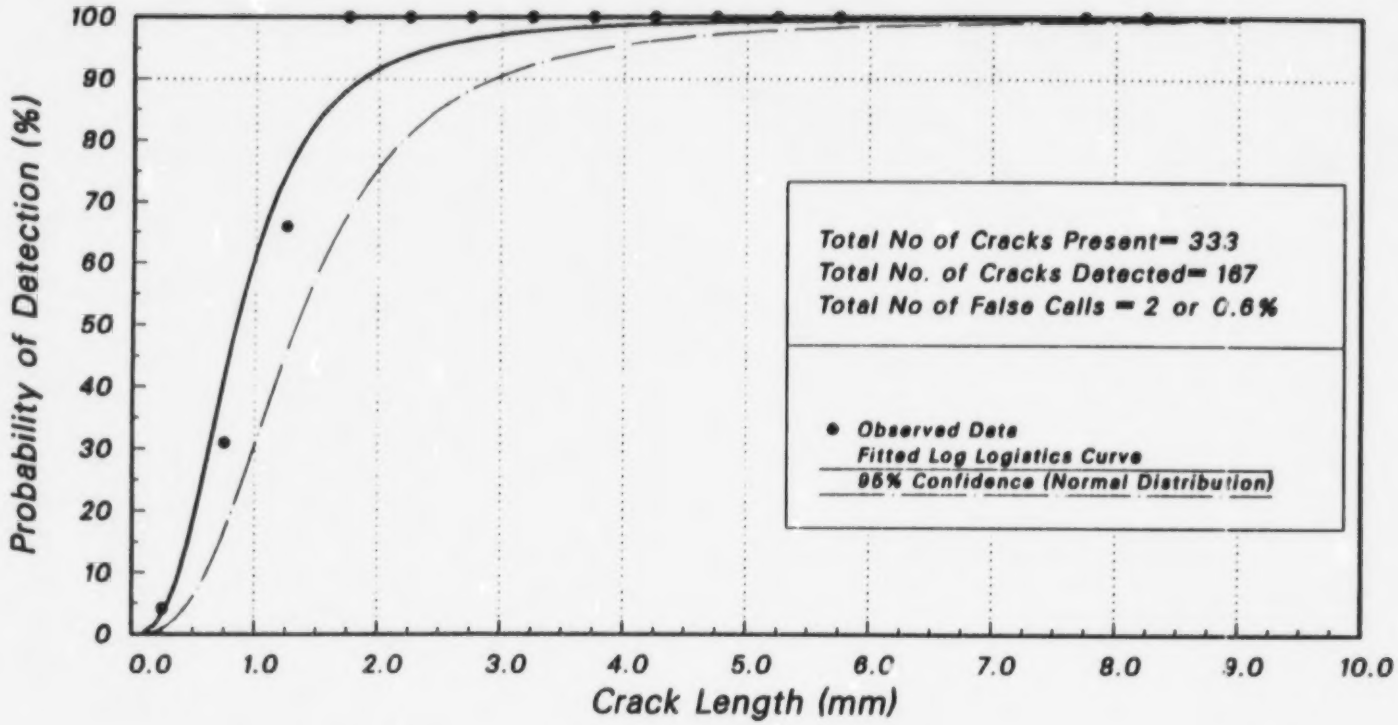

Figure 17: Probability of detection of LCF cracks in compressor discs using ultrasonic leaky wave technique. NAE results using automated C-scan system

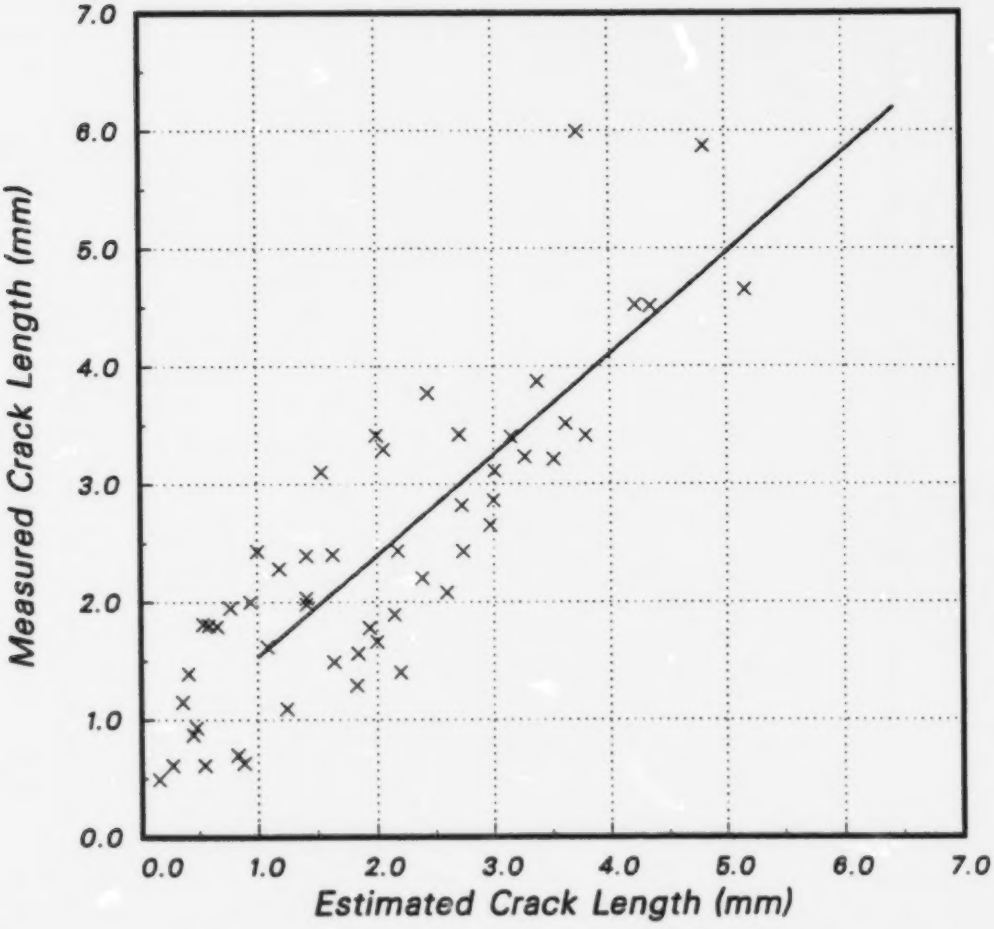

Figure 18: ***A comparison of crack lengths estimated by the liquid penetrant technique (45 minute soaking period) with those measured along the surfaces of the discs using scanning electron microscopy***

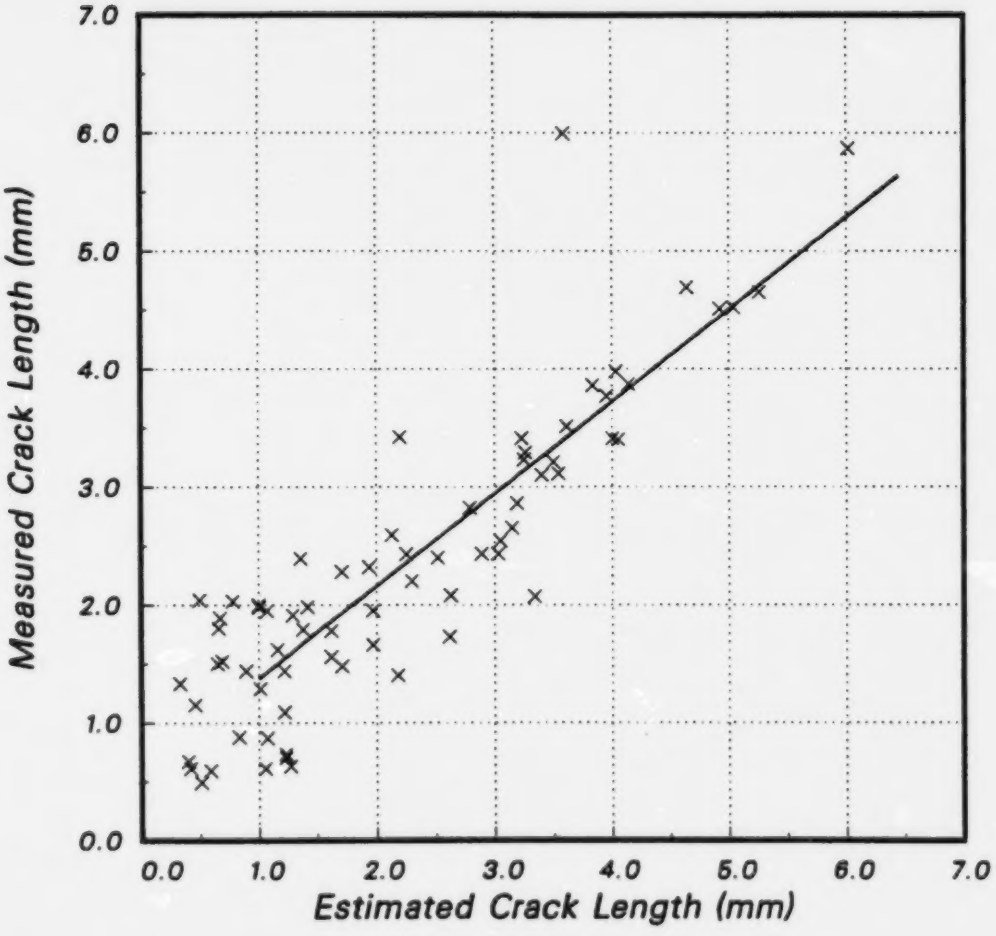

Figure 19: *A comparison of crack lengths estimated by the liquid penetrant technique (60 minute soaking period) with those measured along the surfaces of the discs using scanning electron microscopy*

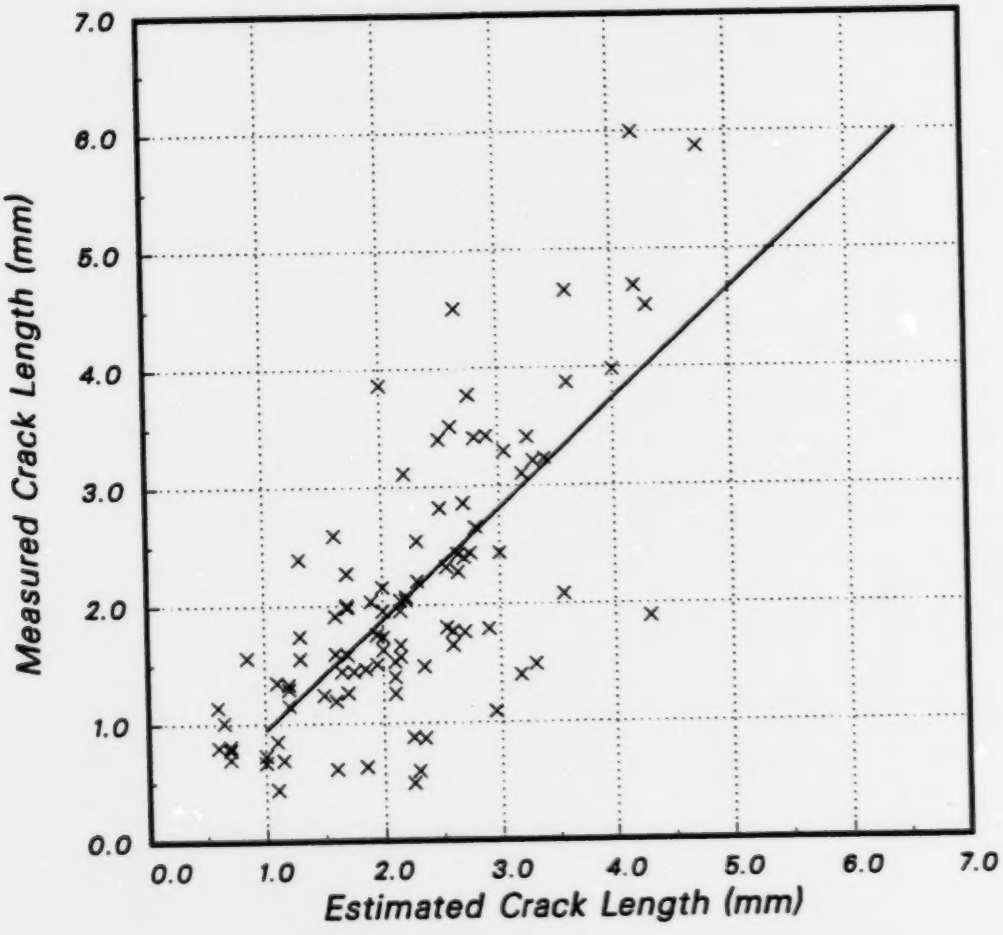

Figure 20: ***A comparison of crack lengths estimated by the ultrasonic leaky waves with those measured along the surfaces of the discs using scanning electron microscopy***

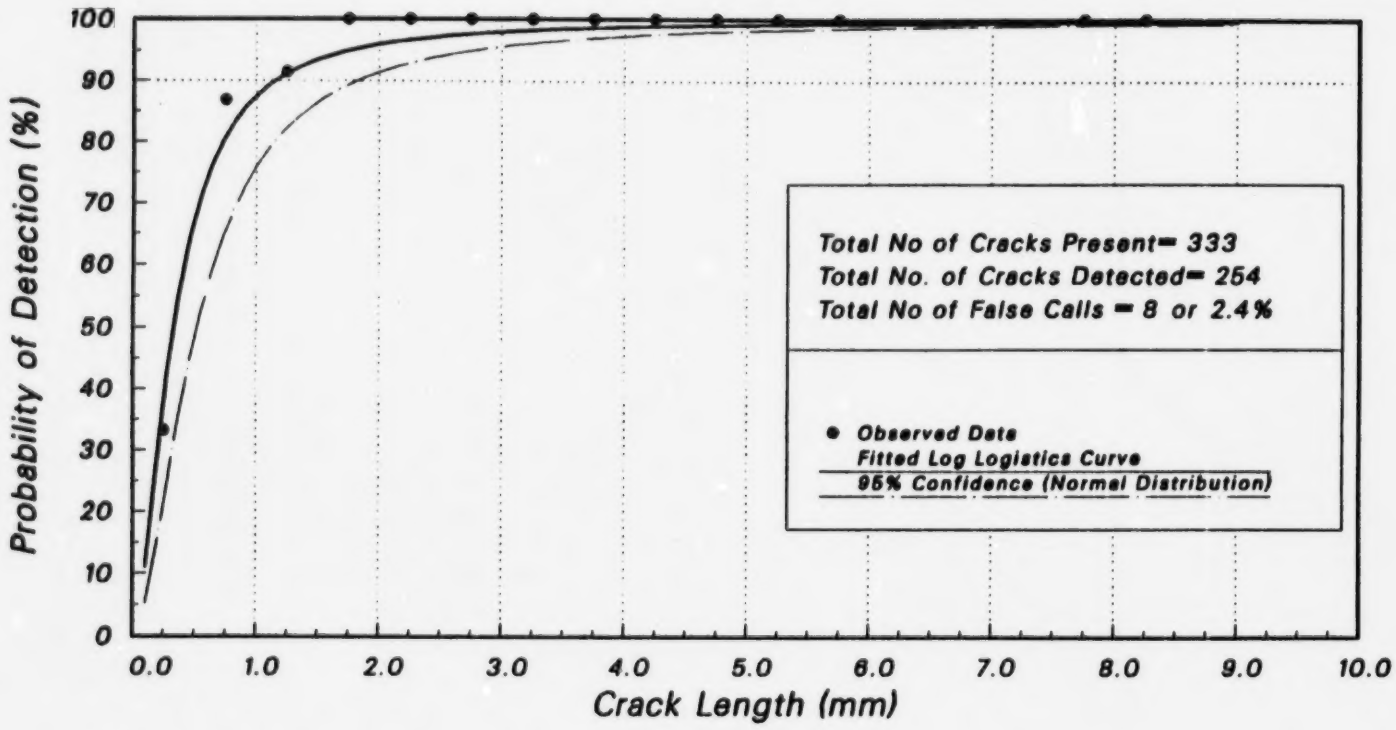

Figure 21: Probability of detection of LCF cracks in compressor discs using manual eddy current technique. AMDU results, high gain setting with the 2.70 mm crack considered as detected

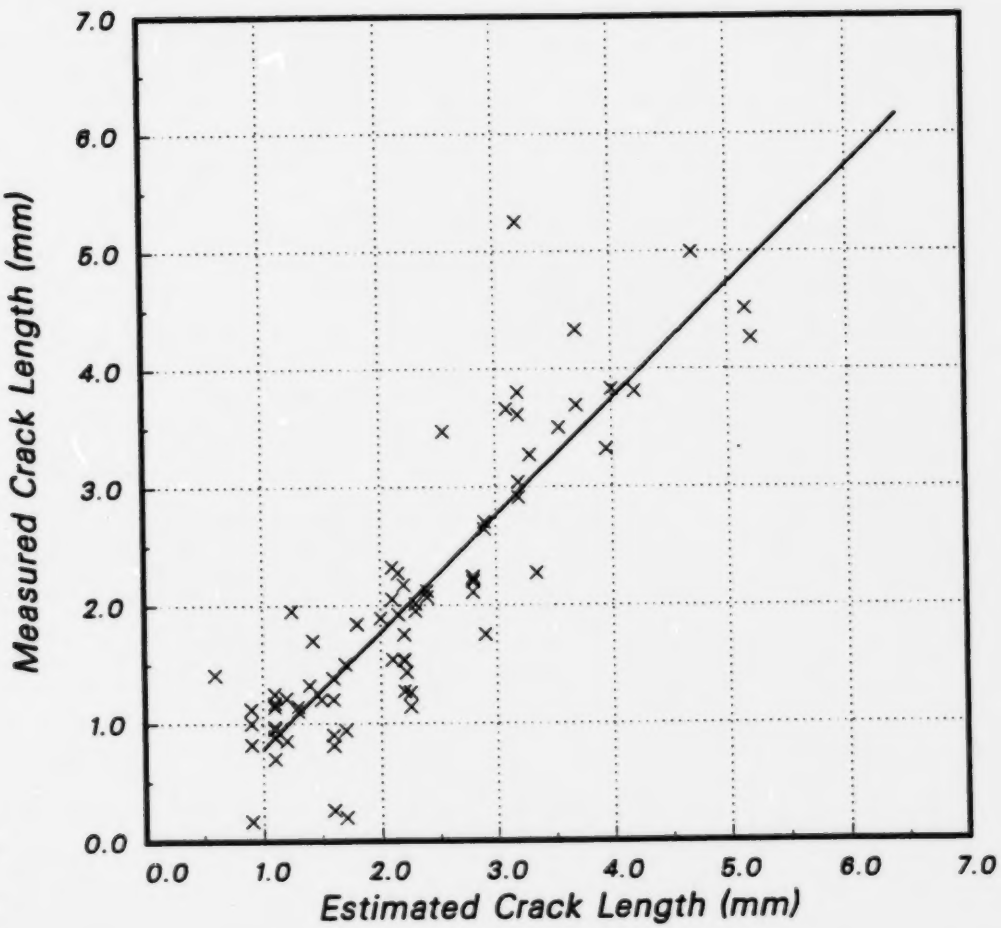

Figure 22: ***A comparison of crack lengths estimated by the ultrasonic leaky waves with maximum crack lengths as measured by scanning electron microscopy***

APPENDIX A

A.1 COMPARISON OF DIFFERENT STATISTICAL DISTRIBUTIONS USED FOR CONFIDENCE BOUNDS

In order to determine the statistical distribution best suited for describing the category 2 type data presented in this study, a number of distributions were used to calculate the 95% lower confidence bound on the log-logistic mean POD line for the different NDI techniques investigated. These distributions included the F-distribution, normal distribution, student t-distribution and the binomial distribution.

The F-, normal and student t-distributions determine the confidence line about the mean line as a whole whereas the binomial distribution uses the actual data points. This appendix presents the equations and methods used to obtain each confidence line.

A.1.1 The Normal Distribution

In the normal distribution, it is assumed that the probability of detection varies normally for a given crack length and that the variance is the same for any crack length[A.1]. The 95% confidence bounds are determined using the following equation:

$$POD_{95\%} = POD_{MEAN} \pm 1.96\, S_{y/x} \tag{A1}$$

where 1.96 is the normal standard variate for a confidence interval of 0.95[A.1] and $S_{y/x}$ is the conditional standard variance given by the following equation:

$$S_{y/x} = \left[\frac{S_{yy} - \frac{S_{xy}^2}{S_{xx}}}{n - 2} \right]^{1/2} \tag{A2}$$

where

$$S_{yy} = \Sigma y^2 - \frac{(\Sigma y)^2}{n} \tag{A3}$$

$$S_{xx} = \Sigma x^2 - \frac{(\Sigma x)^2}{n} \tag{A4}$$

$$S_{xy} = \Sigma xy - \frac{(\Sigma x \Sigma y)}{n} \qquad (A5)$$

This assumption results in a lower bound confidence line which is also a log-logistic curve with the same slope as the POD mean linear regression line but with a different intercept.

A.1.2 The F-distribution

The F-distribution does not assume any underlying distribution of the variation of a variable but is based on the correlation between two variables. Confidence bounds are determined by choosing the desired confidence level, $1 - \alpha$ ($\alpha = 0.05$ in this case), obtain $F_{1-\alpha}$ for two degrees of freedom (N_1, N_2) from Table A.2 and then choosing the x values at which to compute points for drawing the confidence band using the following equations(A.2):

$$Y_c = \overline{Y} = b_1 (x - \overline{x}) \qquad (A6)$$

$$W_1 = \sqrt{2F}\, S_{y/x} \left[\frac{1}{n} + \frac{(x - \overline{x})^2}{S_{xx}}\right]^{1/2} \qquad (A7)$$

where $S_{y/x}$, S_{xx} are given in Equation A2 and

$$b_1 = \frac{S_{xy}}{S_{xx}} \qquad (A8)$$

where S_{xy} is given in Equation A5.

Therefore, the $1 - \alpha$ confidence band for the whole line is determined by:

$$Y_c - W_1 \qquad (A9)$$

A.1.3 The Student t-distribution

The underlying distribution of a student t-distribution is the normal distribution. When the number of points approaches infinity, this distribution becomes the same as the normal distribution. The confidence bounds are calculated in a similar manner to the normal distribution except that the normal standard deviate 1.96 is replaced by some t value which depends on the number of data points. The equation for determining these confidence bounds is as follows:

$$POD_{95\%} = POD_{MEAN} \pm t_{\alpha/2,n-1}\, S_{y/x} \qquad (A10)$$

where $t_{\alpha/2,n-1}$ is obtained from Table A.3 and the $S_{y/x}$ is found from Equation A2.

A.1.4 The Binomial Distribution

With a confidence level of $100(1-\alpha)$, the lower bound on the estimate of P can be calculated as the solution, P_L, to the equation:

$$\alpha = \sum_{i=r}^{n} \frac{n!}{(n-i)!\ i!}\ P_L^{\,i}\ (1-P_L)^{n-i} \qquad (A11)$$

Solutions to this equation have been determined and are presented in Figure A.1.

There are a number of techniques which have been developed to determine the confidence bounds using the binomial distribution. The main difference between these techniques is in the manner in which the crack length intervals are created. The simplest of these methods is known as the Range Interval Method (RIM). In this method, crack length intervals are defined for equal crack lengths across the range of data. However, the lower bound confidence lines which are generated using this method can exhibit an apparent erratic behaviour due to a strong dependency on the sample size (i.e. number of crack lengths contained in each interval) as shown in Figure A.2.

To eliminate this strong dependency on sample size, Yee et al[A.3] recommended the use of the Optimized Probability Method (OPM) which provides the

highest possible lower confidence bounds of all binomial distribution methods. Initially, crack intervals are formed as in the range interval method giving rise to m intervals ranging from 1 through m with the longest cracks in interval 1. The lowest confidence bound on POD, P_L, is calculated first for the data in interval 1, then for the data in intervals 1 and 2 together, then for intervals 1, 2 and 3 and so forth until a lower confidence bound is calculated for the whole data set (i.e. intervals 1 through m inclusive). The group of intervals which give rise to the highest lower confidence bound are then used for the first interval (i.e. the largest crack). Then, the data in interval 1 is eliminated and intervals 2 through m are analyzed in a similar manner. This process continues until confidence bounds for all m intervals are found. The lower 95% confidence bound which result from this method is also shown in Figure A.2. As can be seen from this graph, the confidence line calculated from the Optimized Probability Method is much better behaved than that determined from the Range Interval Method. It should be pointed out however that these better behaved confidence bounds are obtained at the expense of unknown statistical validity of the POD function across all ranges of crack length(A.4).

A.2 RESULTS

Figures A.3 to A.5 show the probability of detection as a function of crack length for the best of the LPI techniques, more sensitive eddy current technique and the ultrasonic leaky wave technique respectively. Each figure illustrates the observed data points, the mean log-logistic curve fitted to the data and three 95% lower confidence bound lines obtained by using the F-distribution and the student t-distribution as well as the normal distribution. The 90% POD/95% confidence limits are given in Table A.1 for all NDI techniques examined.

Figures A.6 to A.8 show the observed data points along with the 95% lower confidence bound lines obtained by using the binomial distribution for the best of the LPI techniques, more sensitive eddy current technique as well as the ultrasonic leaky wave technique, respectively. Both the Range Interval Method and the Optimized Probability Method were used to obtain the confidence line. The resulting 90% POD/95% confidence limits are presented in Table A.1.

A.3 DISCUSSION

Of all the statistical distributions examined, the F-distribution resulted in the smallest limiting crack length (ie. 90%/95% POD limit) for all the NDI techniques examined except for the ultrasonic leaky wave technique which resulted in a crack length of greater than 10 mm. As can be seen in Figure A.5, the confidence line determined by assuming a F-distribution appears to level off at approximately the 50% POD level which is unrealistic since the ultrasonic leaky wave technique detected all cracks greater than 1.5 mm. The reason for this may be due to the fact that only four data points were used for the linear regression analysis. Since an equation could not be readily determined for the F-distribution confidence line and actual points had to be transferred from each regression plot, the resulting 95% lower confidence bound line should only be valid over those points used in the regression analysis. Therefore, the limiting crack length determined for each NDI technique by assuming a F-distribution is not valid since they had to be extrapolated from the POD plots.

On the other hand, both the normal and student t-distributions resulted in an equation for each confidence line and therefore were valid over the entire data set and resulted in more realistic 95% lower confidence bound lines since these lines were tighter about the meanline at the higher crack lenghts. As was pointed out earlier, the normal distribution resulted in slightly tighter confidence bounds than those resulting from the student t-distribution. Only the less sensitive eddy current technique resulted in a limiting crack length of greater than 10 mm for the normal and student t-distribution confidence lines.

The binomial distribution, however, resulted in limiting crack lengths for only the ultrasonic leaky wave technique and the more sensitive eddy current technique and only when the Optimized Probability Method was used. The Range Interval Method, on the other hand, did not result in any limiting crack lengths (all values were greater than 10 mm). In fact, all confidence lines levelled off at the 5% POD level for all the techniques examined even though all cracks were detected at these lengths. This demonstrates the effect that sample size has on this method.

A.4 REFERENCES

A.1 Ang, A., and Tang, W.H., 'Probability Concepts in Engineering Planning and Design', Volume 1 Basic Principles, John Wiley and Sons Inc., New York, 1975.

A.2 Natrella, M.G., 'Experimental Statistics', U.S. National Bureau of Standards, Handbook 91, U.S. Government Printing Office, 1966.

A.3 Yee, B.G.W., Chang, F.H., Couchman, J.C., Lemon, G.H. and Packman, P.F., 'Assessment of NDE Reliability Data', General Dynamics, Fort Worth, Texas, July 1974 - September 1976, NASA-CR-134991, Final Report, October 1976.

A.4 Berens, A.P. and Hovey, P.W., 'Statistical Methods for Estimation Crack Detection Probabilities', Probabilistic Fracture Mechanics and Fatigue Methods: Applications for Structural Design and Maintenance, ASTM STP 798, 1983.

Table A.1: 90% POD/95% Confidence

NDI Technique	F-distribution	Normal Distribution	Student t	RIM	OPM
Ultrasonic Leaky Waves	10	2.90	3.60	10	2.1
Eddy Current 2	7.60	10	10	10	10
Eddy Current 5	2.75	4.10	5.00	10	2.1
LPI (45 min)	6.00	8.35	9.00	10	10
LPI (60 min)	4.90	6.20	6.80	10	10
LPI (Orenda)	5.00	6.40	6.90	10	10

n_1 = degrees of freedom for numerator

n_2 = degrees of freedom for denominator

n_2 \ n_1	1	2	3	4	5	6	7	8	9	10	12	15	20	24	30	40	60	120	∞
1	161.4	199.5	215.7	224.6	230.2	234.0	236.8	238.9	240.5	241.9	243.9	245.9	248.0	249.1	250.1	251.1	252.2	253.3	254.3
2	18.51	19.00	19.16	19.25	19.30	19.33	19.35	19.37	19.38	19.40	19.41	19.43	19.45	19.45	19.46	19.47	19.48	19.49	19.50
3	10.13	9.55	9.28	9.12	9.01	8.94	8.89	8.85	8.81	8.79	8.74	8.70	8.66	8.64	8.62	8.59	8.57	8.55	8.53
4	7.71	6.94	6.59	6.39	6.26	6.16	6.09	6.04	6.00	5.96	5.91	5.86	5.80	5.77	5.75	5.72	5.69	5.66	5.63
5	6.61	5.79	5.41	5.19	5.05	4.95	4.88	4.82	4.77	4.74	4.68	4.62	4.56	4.53	4.50	4.46	4.43	4.40	4.36
6	5.99	5.14	4.76	4.53	4.39	4.28	4.21	4.15	4.10	4.06	4.00	3.94	3.87	3.84	3.81	3.77	3.74	3.70	3.67
7	5.59	4.74	4.35	4.12	3.97	3.87	3.79	3.73	3.68	3.64	3.57	3.51	3.44	3.41	3.38	3.34	3.30	3.27	3.23
8	5.32	4.46	4.07	3.84	3.69	3.58	3.50	3.44	3.39	3.35	3.28	3.22	3.15	3.12	3.08	3.04	3.01	2.97	2.93
9	5.12	4.26	3.86	3.63	3.48	3.37	3.29	3.23	3.18	3.14	3.07	3.01	2.94	2.90	2.86	2.83	2.79	2.75	2.71
10	4.96	4.10	3.71	3.48	3.33	3.22	3.14	3.07	3.02	2.98	2.91	2.85	2.77	2.74	2.70	2.66	2.62	2.58	2.54
11	4.84	3.98	3.59	3.36	3.20	3.09	3.01	2.95	2.90	2.85	2.79	2.72	2.65	2.61	2.57	2.53	2.49	2.45	2.40
12	4.75	3.89	3.49	3.26	3.11	3.00	2.91	2.85	2.80	2.75	2.69	2.62	2.54	2.51	2.47	2.43	2.38	2.34	2.30
13	4.67	3.81	3.41	3.18	3.03	2.92	2.83	2.77	2.71	2.67	2.60	2.53	2.46	2.42	2.38	2.34	2.30	2.25	2.21
14	4.60	3.74	3.34	3.11	2.96	2.85	2.76	2.70	2.65	2.60	2.53	2.46	2.39	2.35	2.31	2.27	2.22	2.18	2.13
15	4.54	3.68	3.29	3.06	2.90	2.79	2.71	2.64	2.59	2.54	2.48	2.40	2.33	2.29	2.25	2.20	2.16	2.11	2.07
16	4.49	3.63	3.24	3.01	2.85	2.74	2.66	2.59	2.54	2.49	2.42	2.35	2.28	2.24	2.19	2.15	2.11	2.06	2.01
17	4.45	3.59	3.20	2.96	2.81	2.70	2.61	2.55	2.49	2.45	2.38	2.31	2.23	2.19	2.15	2.10	2.06	2.01	1.96
18	4.41	3.55	3.16	2.93	2.77	2.66	2.58	2.51	2.46	2.41	2.34	2.27	2.19	2.15	2.11	2.06	2.02	1.97	1.92
19	4.38	3.52	3.13	2.90	2.74	2.63	2.54	2.48	2.42	2.38	2.31	2.23	2.16	2.11	2.07	2.03	1.98	1.93	1.88
20	4.35	3.49	3.10	2.87	2.71	2.60	2.51	2.45	2.39	2.35	2.28	2.20	2.12	2.08	2.04	1.99	1.95	1.90	1.84
21	4.32	3.47	3.07	2.84	2.68	2.57	2.49	2.42	2.37	2.32	2.25	2.18	2.10	2.05	2.01	1.96	1.92	1.87	1.81
22	4.30	3.44	3.05	2.82	2.66	2.55	2.46	2.40	2.34	2.30	2.23	2.15	2.07	2.03	1.98	1.94	1.89	1.84	1.78
23	4.28	3.42	3.03	2.80	2.64	2.53	2.44	2.37	2.32	2.27	2.20	2.13	2.05	2.01	1.96	1.91	1.86	1.81	1.76
24	4.26	3.40	3.01	2.78	2.62	2.51	2.42	2.36	2.30	2.25	2.18	2.11	2.03	1.98	1.94	1.89	1.84	1.79	1.73
25	4.24	3.39	2.99	2.76	2.60	2.49	2.40	2.34	2.28	2.24	2.16	2.09	2.01	1.96	1.92	1.87	1.82	1.77	1.71
26	4.23	3.37	2.98	2.74	2.59	2.47	2.39	2.32	2.27	2.22	2.15	2.07	1.99	1.95	1.90	1.85	1.80	1.75	1.69
27	4.21	3.35	2.96	2.73	2.57	2.46	2.37	2.31	2.25	2.20	2.13	2.06	1.97	1.93	1.88	1.84	1.79	1.73	1.67
28	4.20	3.34	2.95	2.71	2.56	2.45	2.36	2.29	2.24	2.19	2.12	2.04	1.96	1.91	1.87	1.82	1.77	1.71	1.65
29	4.18	3.33	2.93	2.70	2.55	2.43	2.35	2.28	2.22	2.18	2.10	2.03	1.94	1.90	1.85	1.81	1.75	1.70	1.64
30	4.17	3.32	2.92	2.69	2.53	2.42	2.33	2.27	2.21	2.16	2.09	2.01	1.93	1.89	1.84	1.79	1.74	1.68	1.62
40	4.08	3.23	2.84	2.61	2.45	2.34	2.25	2.18	2.12	2.08	2.00	1.92	1.84	1.79	1.74	1.69	1.64	1.58	1.51
60	4.00	3.15	2.76	2.53	2.37	2.25	2.17	2.10	2.04	1.99	1.92	1.84	1.75	1.70	1.65	1.59	1.53	1.47	1.39
120	3.92	3.07	2.68	2.45	2.29	2.17	2.09	2.02	1.96	1.91	1.83	1.75	1.66	1.61	1.55	1.50	1.43	1.35	1.25
∞	3.84	3.00	2.60	2.37	2.21	2.10	2.01	1.94	1.88	1.83	1.75	1.67	1.57	1.52	1.46	1.39	1.32	1.22	1.00

Table A.2: . Percentiles of the F-distribution

$F_{.95(n_1,n_2)}$

f \ p	0.750	0.900	0.950	0.975	0.990	0.995	0.999
1	1.000	3.078	6.314	12.706	31.821	63.657	318
2	0.816	1.886	2.920	4.303	6.965	9.925	22.3
3	0.765	1.638	2.353	3.182	4.541	5.841	10.2
4	0.741	1.533	2.132	2.776	3.747	4.604	7.173
5	0.727	1.476	2.015	2.571	3.365	4.032	5.893
6	0.718	1.440	1.943	2.447	3.143	3.707	5.208
7	0.711	1.415	1.895	2.365	2.998	3.499	4.785
8	0.706	1.397	1.860	2.306	2.896	3.355	4.501
9	0.703	1.383	1.833	2.262	2.821	3.250	4.297
10	0.700	1.372	1.812	2.228	2.764	3.169	4.144
11	0.697	1.363	1.796	2.201	2.718	3.106	4.025
12	0.695	1.356	1.782	2.179	2.681	3.055	3.930
13	0.694	1.350	1.771	2.160	2.650	3.012	3.852
14	0.692	1.345	1.761	2.145	2.624	2.977	3.787
15	0.691	1.341	1.753	2.131	2.602	2.947	3.733
16	0.690	1.337	1.746	2.120	2.583	2.921	3.686
17	0.689	1.333	1.740	2.110	2.567	2.898	3.646
18	0.688	1.330	1.734	2.101	2.552	2.878	3.610
19	0.688	1.328	1.729	2.093	2.539	2.861	3.579
20	0.687	1.325	1.725	2.086	2.528	2.845	3.552
21	0.686	1.323	1.721	2.080	2.518	2.831	3.527
22	0.686	1.321	1.717	2.074	2.508	2.819	3.505
23	0.685	1.319	1.714	2.069	2.500	2.807	3.485
24	0.685	1.318	1.711	2.064	2.492	2.797	3.467
25	0.684	1.316	1.708	2.060	2.485	2.787	3.450
26	0.684	1.315	1.706	2.056	2.479	2.779	3.435
27	0.684	1.314	1.703	2.052	2.473	2.771	3.421
28	0.683	1.313	1.701	2.048	2.467	2.763	3.408
29	0.683	1.311	1.699	2.045	2.462	2.756	3.396
30	0.683	1.310	1.697	2.042	2.457	2.750	3.385
40	0.681	1.303	1.684	2.021	2.423	2.704	3.307
60	0.679	1.296	1.671	2.000	2.390	2.660	3.232
120	0.677	1.289	1.658	1.980	2.358	2.617	3.160
∞	0.674	1.282	1.645	1.960	2.326	2.576	3.090

Table A.3 : Percentiles of the t-distribution

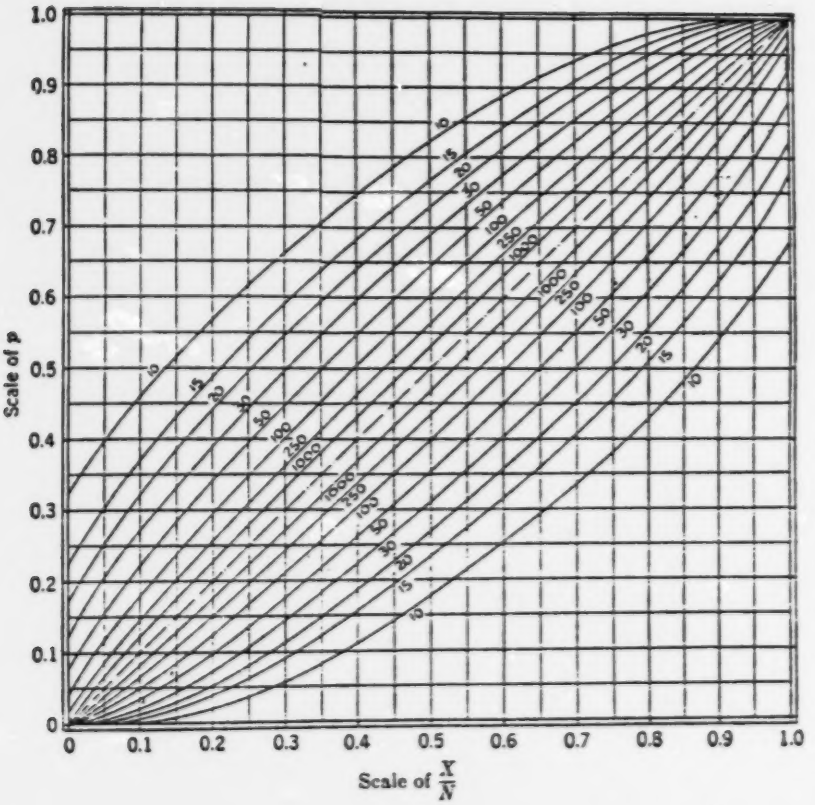

Figure A.1: Percentiles of the binomial distribution

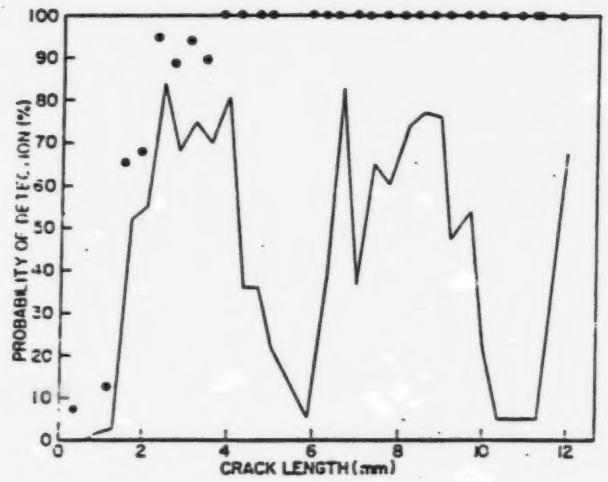

Figure A.2a: Example POD confidence limits using the Range Interval Method[A.4]

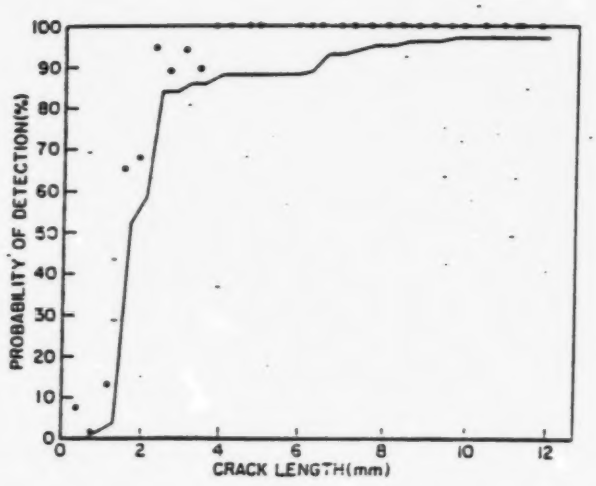

Figure A.2b: Example POD confidence limits using the Optimized Probability Method[A.4]

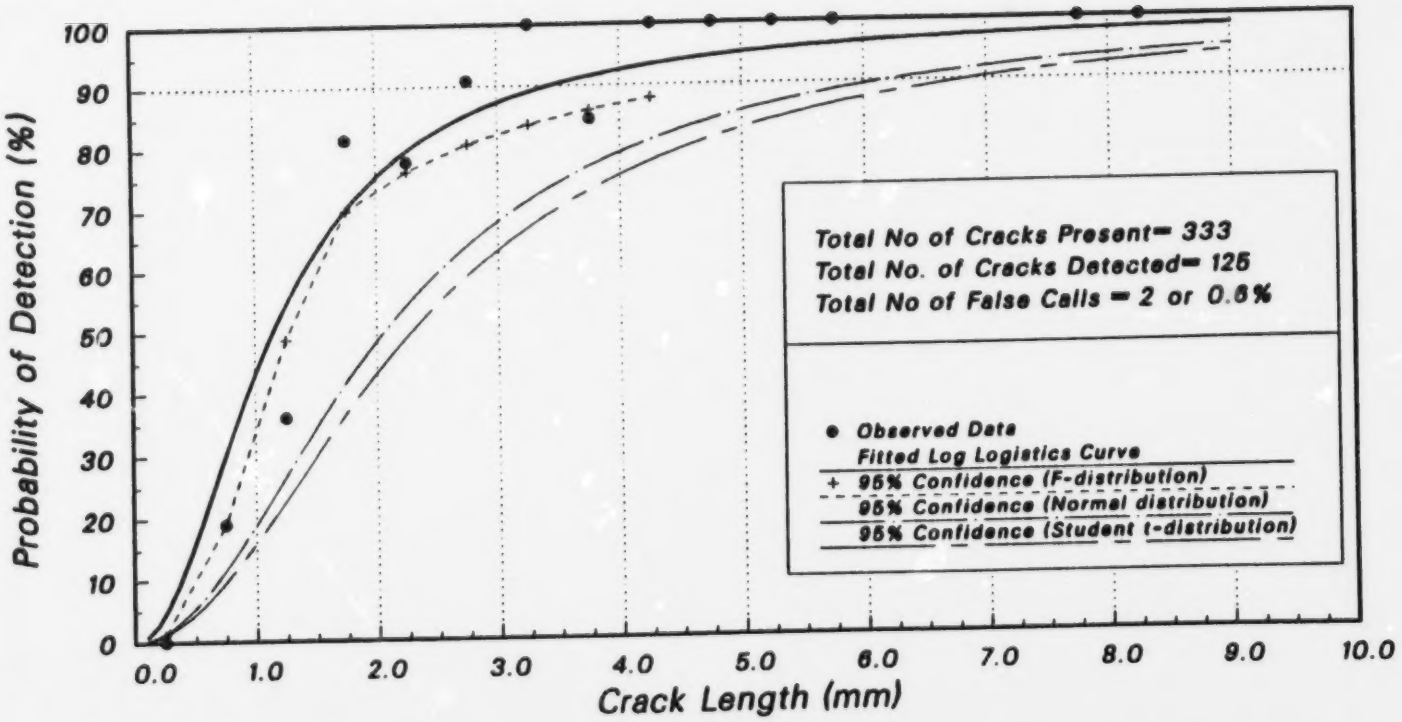

Figure A.3: Probability of detection of LCF cracks in compressor discs using the liquid penetrant inspection technique with a 60 minute soaking period and 95% confidence lines determined by the F-distribution, the normal distribution and the student t-distribution

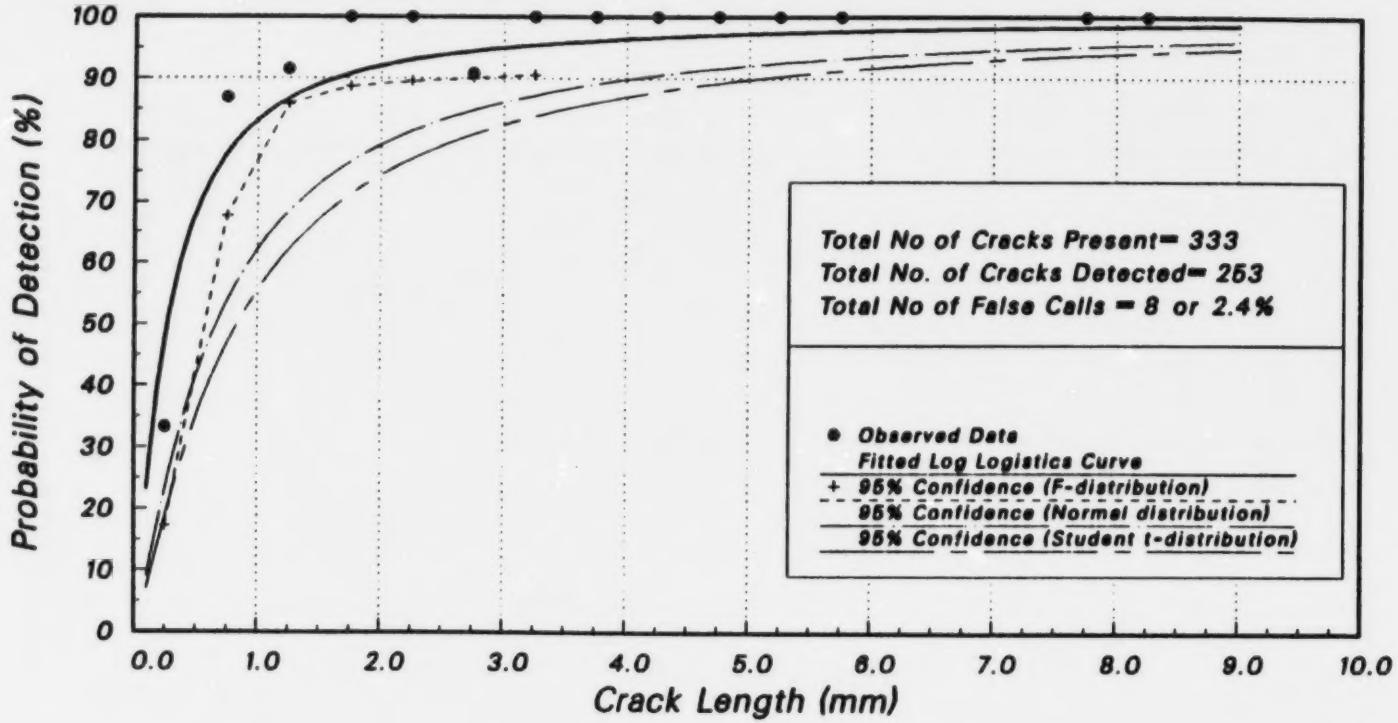

Figure A.4: Probability of detection of LCF cracks in compressor discs using the eddy current inspection technique with a gain setting of 5 and 95% confidence lines determined by the F-distribution, the normal distribution and the student t-distribution

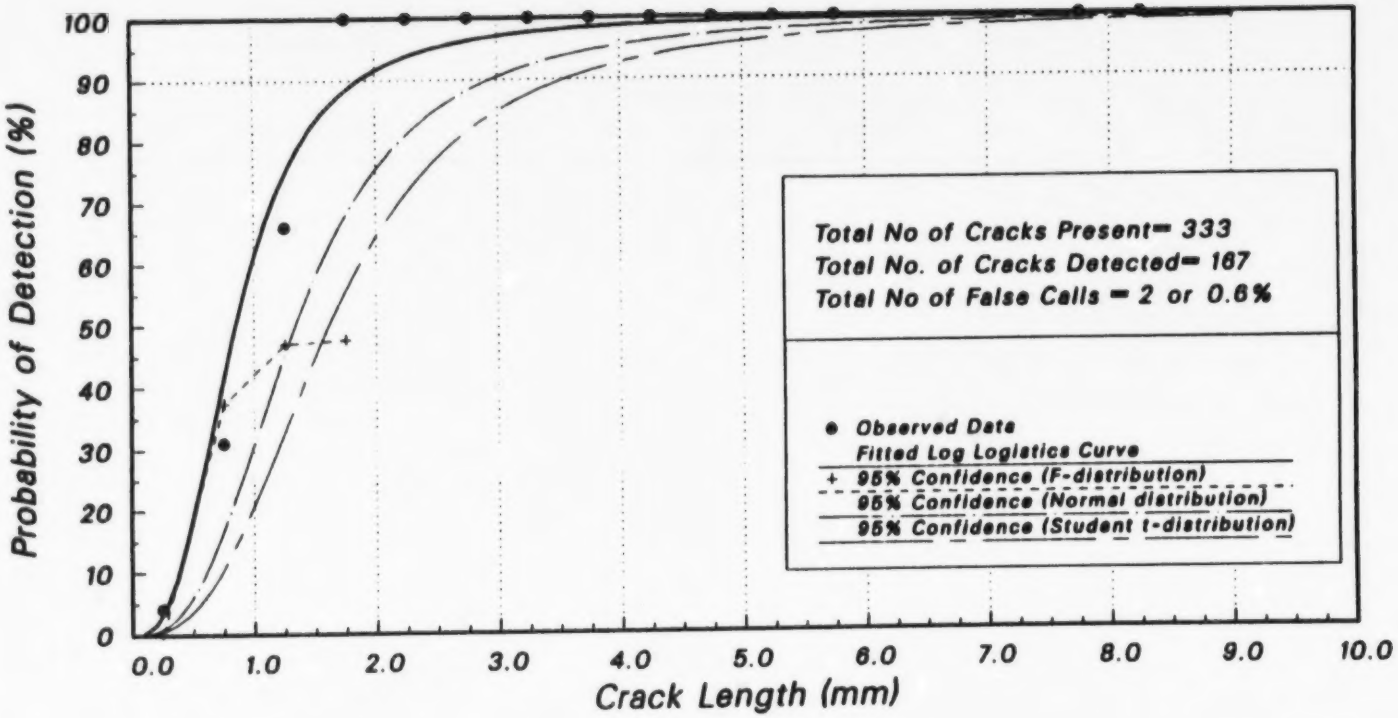

Figure A.5: Probability of detection of LCF cracks in compressor discs using the ultrasonic leaky wave technique with 95% confidence lines determined by the F-distribution, the normal distribution and the student t-distribution

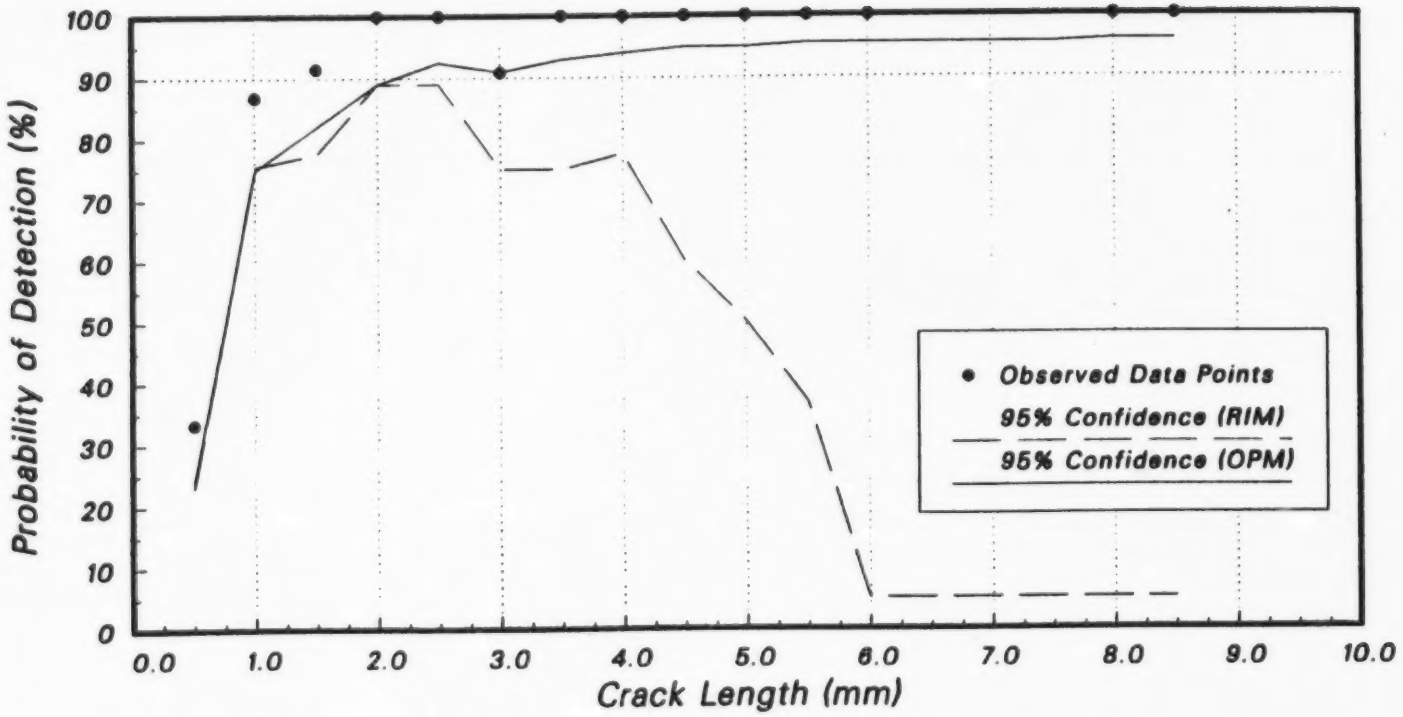

Figure A.6: Probability of detection for the eddy current inspection technique with a gain setting of 5 and with 95% confidence lines determined by the binomial distribution

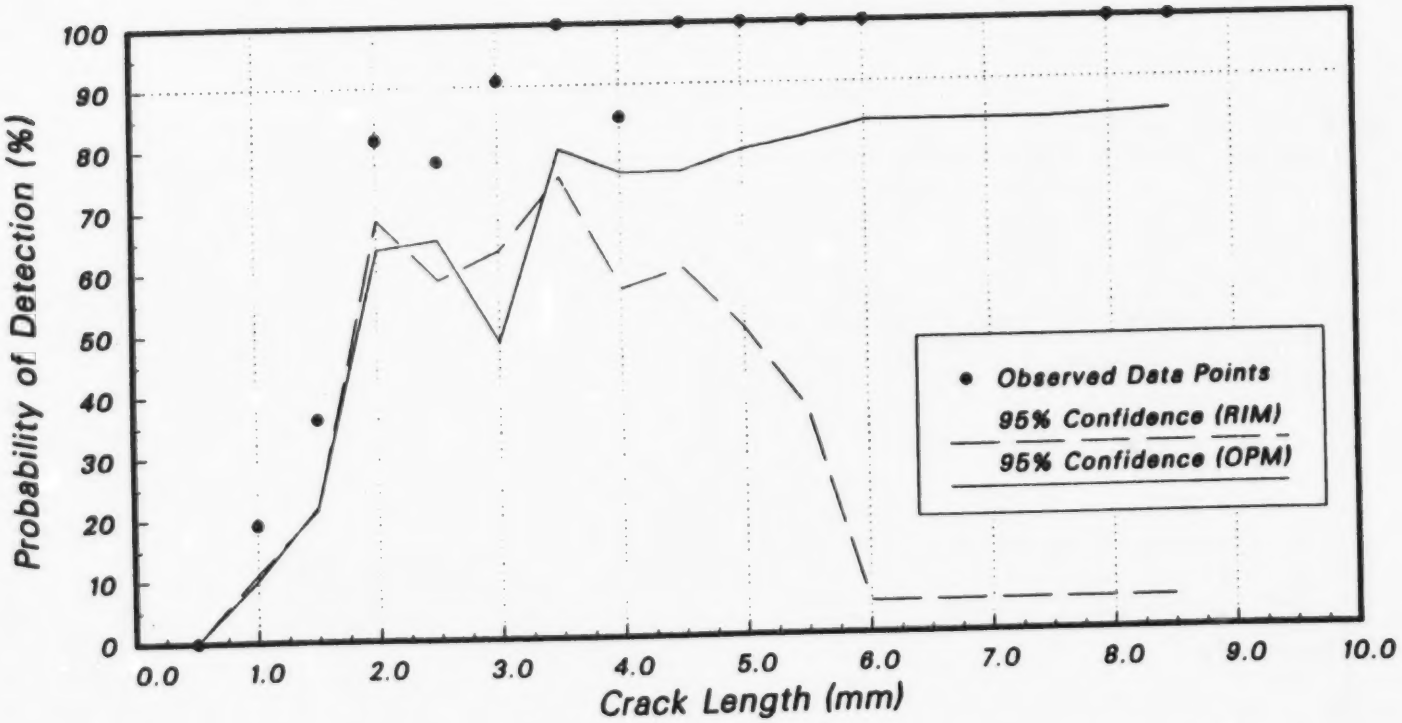

Figure A.7: ***Probability of detection for the liquid penetrant inspection technique with a 60 minute soaking period and with 95% confidence lines determined by the binomial distribution***

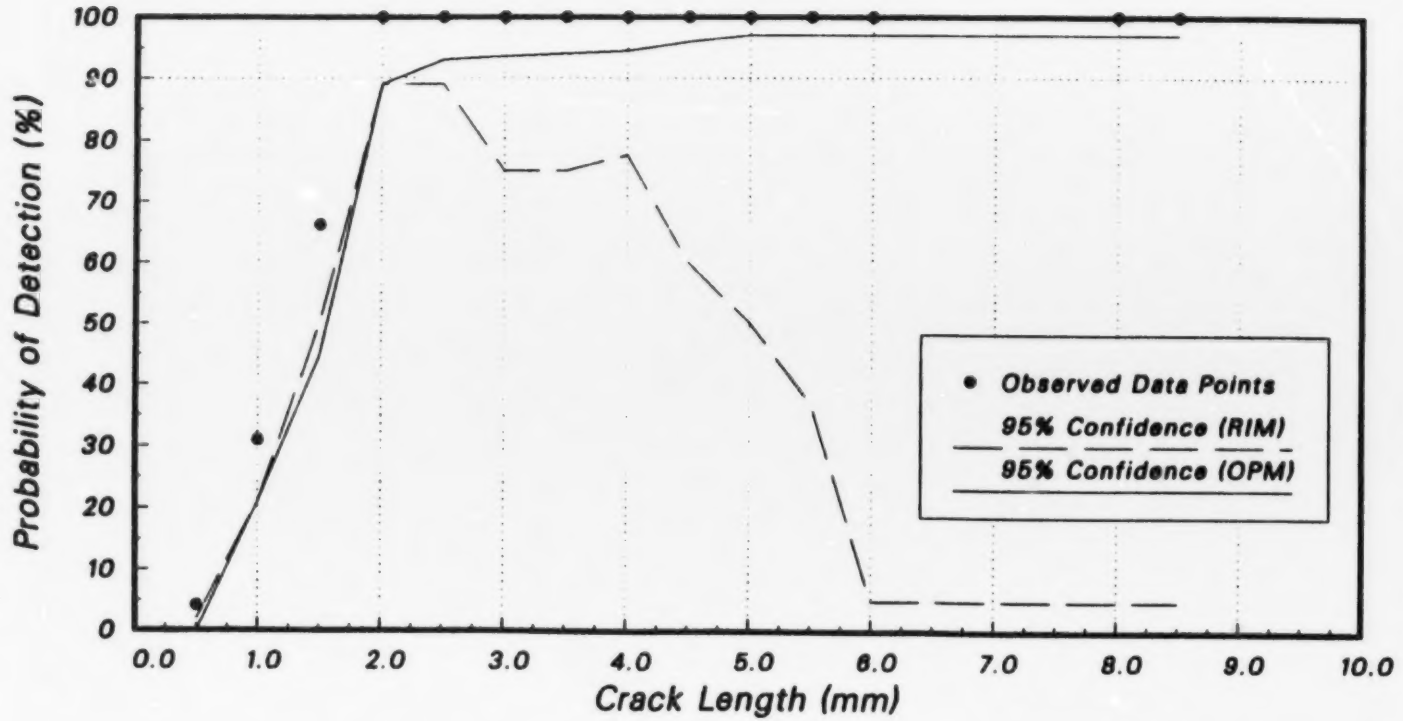

Figure A.8: Probability of detection for the ultrasonic leaky wave technique with 95% confidence lines determined by the binomial distribution